Universidad
Carlos III de Madrid

SCHOOL OF ENGINEERING
DEPARTAMENT OF THERMAL AND FLUIDS ENGINEERING

BACHELOR THESIS
BACHELOR'S DEGREE IN MECHANICAL ENGINEERING

Study of the effect of non- uniform flow distribution in the transient response of a system of flat plate solar collectors for hot water service

Author: Dña. María Eugenia de Juan von Wichmann
Tutor: D. Ricardo Alberto López Silva

September 2016

ACKNOWLEDGEMENTS

I would like to express my sincere gratitude to all the people who accompanied me during these past years and were involved in the realization of this accomplishment, with a special dedication to the following:

First of all, to my family, who always encouraged me to keep moving forward and supported all my decisions. Especially to my parents for always being there for me: my mother, who knows how to cheer me up when times are a bit rough; and my father and mentor, who helps me see the bigger picture and calms me when I am feeling overwhelmed. I would never have achieved this without you and for that I am extremely grateful.

To my friends and main support at the university, Vero and Verito. Thank you for understanding and helping me grow as a person. It has been a pleasure sharing all these years with you.

To my fellow mechanical engineers who were always willing to help me overcome the difficulties that rose from this degree. Particularly, Elena and Andrés, who made me see the best outcomes out of the worst situations and managed to make this trajectory a lot easier.

Finally, to my tutor, for making this project possible and working side to side with me these past months.

TABLE OF CONTENTS

INDEX OF FIGURES

INDEX OF TABLES

NOMENCLATURE

HWS	Hot Water Service
DBHE	"*Documento Básico HE de Ahorro de energía*"
CTE	*"Código Técnico de la Edificación"*
β_{OPT}	Optimum tilt of the solar collector (°)
H''_{OPT}	Solar radiation for a plane with optimum tilt $\left({}^{Wh}/_{m^2 \cdot day}\right)$
T_a	Average daily ambient temperature (°C)
H	Solar irradiance in Madrid $\left({}^{Wh}/_{m^2 \cdot day}\right)$
$D(T)$	Demand of HWS at temperature T $\left({}^{l}/_{day}\right)$
$D_i(T)$	Demand of HWS for month "i" at temperature T $\left({}^{l}/_{month}\right)$
D_i(60°C)	Demand of HWS for month "i" at 60°C $\left({}^{l}/_{month}\right)$
T	Final temperature (°C)
T_i	Mean minimum temperature of network water (°C)
$\dot{m}_c$	Annual average flow of consumption $\left({}^{kg}/_{s}\right)$
f	Minimum solar contribution (%)
Q_{HWS}	Heat transferred to the HWS (kW)
c_p	Specific heat capacity of water $\left({}^{J}/_{kgK}\right)$
T_{cons}	Temperature of consumption of water (°C)

T_{net}	Mean minimum temperature of network water (°C)
Q_{min}	Minimum heat provided by the HWS system (kW)
β	Tilt angle (°)
α	Azimuth's angle (°)
ϕ	Latitude
β_{max}	Maximum tilt angle (°)
β_{min}	Minimum tilt angle (°)
$\dot{m}_s$	Water flow in the first circuit $\left({}^{kg}/_{s}\right)$
ΔT_s	Temperature difference in the solar collector (°C)
η	Efficiency of the solar collector
q_{max}	Maximum possible heat rate in a heat exchanger
C_{min}	Smallest heat capacity rate of either fluid in the heat exchanger
$\left(T_{h,i} - T_{c,i}\right)$	Maximum temperature difference in a heat exchanger
ε	Effectiveness of a heat exchanger
q	Actual heat transfer rate for a heat exchanger
C_h	Heat capacity rate for the hot fluid in a heat exchanger
C_c	Heat capacity rate for the cold fluid in a heat exchanger
T_{co}	Outlet temperature of the solar collector (°C)
T_{ci}	Inlet temperature of the solar collector (°C)

$A_{c,total}$	Total area of the solar collectors (m^2)
Q''	Global solar radiation $\left({}^{kWh}/_{m^2 \cdot day}\right)$
$U_L(T_{pm} - T_a)$	Heat losses at the walls of the collector $\left({}^{W}/_{m^2}\right)$
T_{pm}	Mean temperature of the collector (°C)
U_L	Total heat loss coefficient $\left({}^{W}/_{m^2 °C}\right)$
U_t	Top loss coefficient $\left({}^{W}/_{m^2 °C}\right)$
T_p	Plate's temperature (°C)
N	Number of transparent glass covers
σ	Stefan- Boltzmann constant $\left(5.67 \cdot 10^{-8}\, {}^{W}/_{m^2 K^4}\right)$
h_w	Convective heat transfer coefficient due to wind $\left({}^{W}/_{m^2 °C}\right)$
ϵ_p	Thermal emissivity of the absorbing plate surface
ϵ_g	Thermal emissivity of the cover
u	Wind's velocity $({}^{m}/_{s})$
W_{total}	Total width of the connected solar collectors (m)
L	Length of one solar collector (m)
N_c	Number of solar collectors
W_c	Width of one flat plate solar collector (m)
q_u	Useful heat rate (kW)
d	Separation between tubes (m)

D_i	Tube inner diameter (m)
n	Number of tubes per solar collector
$\dot{m}_i$	Water flow per tube in a solar collector $\left({}^{kg}/_{s \cdot tube}\right)$
W_i	Width per tube in a solar collector $\left({}^{m}/_{tube}\right)$
F'	Local efficiency factor of the collector
D_o	Tube outer diameter (m)
h_f	Convective coefficient inside the tube $\left({}^{W}/_{m^2K}\right)$
F	Fin's efficiency
C_b	Conductance in the union between the tube and the plate
Re	Reynold's number
Nu	Nusselt's number
ρ_w	Density of water $\left(1000\ {}^{kg}/_{m^3}\right)$
u	Velocity of water $({}^{m}/_{s})$
μ	Dynamic viscosity of water $(Pa \cdot s)$
Pr	Prandtl parameter for water
k_{abs}	Thermal conductivity of the absorber plate $\left({}^{W}/_{mK}\right)$
g	Welding between the tube and the absorber plate (m)
δ_{abs}	Absorber's thickness (m)

$\frac{dE}{dt}$	Change in the internal energy
$\dot{Q}_{in}$	Heat transfer rate into the system from the boundaries
$\dot{Q}_{out}$	Heat transfer rate out of the system from the boundaries
$\dot{Q}_{irr}$	Heat absorbed from solar irradiance
δ_g	Glass cover's thickness
α	Absorption coefficient
p	Tube pitch
Δz	Spatial size of control volume
$\dot{Q}_{ac}$	Heat transferred by convection from the working fluid circulating inside the collector
$h_{c,am-g}$	Heat transfer coefficient between the ambient and the cover
$T_{a,i}$	Temperature of the air inside the solar collector
T_g	Temperature of the glass cover
$\dot{Q}_{c,ext}$	Natural convection to the surroundings
$\dot{Q}_{r,ext}$	Heat radiated to the surroundings by radiation
T_{am}	Ambient temperature
$h_{r,ext}$	Heat transfer coefficient by radiation to the surroundings
c_g	Specific heat capacity of glass
ρ_g	Density of the glass cover

V_g	Volume of the glass cover
$\frac{dT_g}{dt}$	Variation of temperature of the glass cover with time
$\delta_{a,i}$	Air gap's thickness
$c_{a,i}(T_{a,i})$	Specific heat capacity of air inside the collector (temperature dependent)
$\rho_{a,i}(T_{a,i})$	Density of air inside the collector (temperature dependent)
$V_{a,i}$	Volume of air inside the collector
$\frac{dT_{a,i}}{dt}$	Variation of air temperature inside the collector with time
$h_{c,g-abs}$	Heat transfer coefficient between the cover and the absorber
T_{abs}	Temperature of the absorber
$(\eta\alpha)$	Effective transmittance- absorption coefficient
k_{in}	Insulation's thermal conductivity
δ_{in}	Insulation's thickness
T_{in}	Temperature at the insulation zone
$h_{c,f}$	Heat transfer coefficient of the working fluid
$c_{abs}(T_{abs})$	Specific heat capacity of the absorber plate (temperature dependent)
$\rho_{abs}(T_{abs})$	Density of the absorber (temperature dependent)
V_{abs}	Absorber's volume
$\frac{dT_{abs}}{dt}$	Variation of the absorber plate temperature with time

δ_{in}	Insulation's thickness
c_{in}	Specific heat capacity of the insulation material
ρ_{in}	Density of the insulation material
V_{in}	Volume of insulation
$\frac{dT_{in}}{dt}$	Variation of temperature of the insulation with time
$h_{c,in-am}$	Heat transfer coefficient between the insulation and the ambient
$c_f(T_f)$	Specific heat capacity of the working fluid (temperature dependent)
$\rho_f(T_f)$	Density of the absorber (temperature dependent)
A	Pipe's cross sectional area
$\frac{\delta T_f}{\delta t}$	Variation of the fluid's temperature with time
$h_{c,f}$	Heat transfer coefficient of the working fluid
$\dot{m}_f$	Mass flow rate of the working fluid
$\frac{\delta T_f}{\delta z}$	Variation of the fluid's temperature in the direction of the flow
C_{HWS}	Heat capacity rate in circuit 2
C_{solar}	Heat capacity rate in circuit 1
ϕ	Non-uniformity parameter
$\bar{\beta}$	Average flow ratio for the total tubes
β_i	Flow ratio for the *ith* tube

ABSTRACT

Flows in manifolds are extensively encountered in diverse fields of engineering, solar collectors among others. The division of fluids into streamlines by means of a manifold causes pressure changes in the headers due to wall friction and changing fluid momentum, which leads to non- uniformity distribution of flow and thus, a decrease in the collector's efficiency.

In this project a numerical analysis of the flow distribution in a flat plate solar collector has been developed. The solution of the mathematical model was found with the use of the finite difference; thus, a computational code in Matlab was developed.

Due to the difficulties of making experimental measurements, a hypothetical instantaneous Hot Water Service (HWS) system located in Leganés (Spain), consisting of a flat plate solar collector and a heat exchanger, was developed based on the regulations established in the *"Código Técnico de la Edificación" (CTE)*.

Once the necessary demand and flow of consumption for the HWS system was obtained, the flat plate solar collector was dimensioned according to the requirements of the system.

Finally, all parameters found (mass flows, geometry of the solar collector and temperatures) are used as boundary conditions of the mathematical model, in that sense a study of the flow distribution inside the solar collector is conducted.

1 INTRODUCTION

Manifold arrangements for flow distribution consist in the distribution of a fluid through a large fluid stream into several smaller streams connected at right angles to another large discharge stream (1). Flows in manifolds are extensively encountered in diverse fields of engineering, including fuel cells, microchannels and solar collectors among others (2).

This type of configurations can present problems of non- uniformity distribution of flow, that is, the mass flow is not equally distributed through the pipes of the solar collector, resulting in an unbalance system, which consequently leads to a decrease in the collector's efficiency.

The uniformity of flow rates among the parallel pipes in a solar collector (manifold) is governed by fluid pressure variations inside the entrance and discharge headers. The greater the pressure drop across the smaller pipes and the smaller the smaller the pressure changes inside the headers, the more uniform the flow will be (1). Theory of flow distribution and pressure drop is hence important to predict the performance and efficiency of manifold systems (2).

The manifolds can be arranged in different manners, affecting as well the velocity and pressure distributions. They are classified according to the direction of the fluid inside the manifold, into combined, divided, "U" and "Z" types, being the two latter the basic ones. Figure 1.1 shows "U" and "Z" manifold distribution system arrangements in conduits (3).

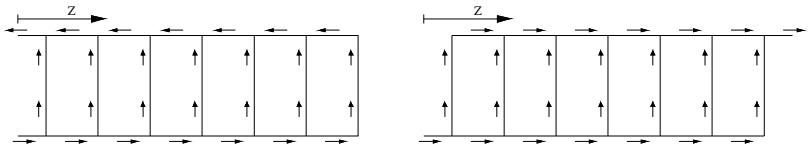

Figure 1.1. "U" type (left) and "Z" type (right) arrangements

Three different approaches have been used in the past 50 years to study this behavior (3):

i. *Computational Fluid Mechanics (CFD)*: Solving 2-D or 3-D momentum, energy, mass and state equations with turbulence models for closing the problem. Although it does not require flow coefficients, it is unsuitable for optimizing geometrical configurations due to its elevated cost (2).

ii. *Discrete Models:* 1-D formulation considering the mean values for velocity and pressure at each section (flow considered to be continuously branched

along a manifold) while adding coefficients to ensure an accurate approximation of the model to the real flow.

iii. *Discrete Models:* Particular cases of the governing equations of some discrete models which give a simplify view of the distribution of the fluid and pressure losses.

One of the most extended analytical models includes the one proposed by *M. K. Bassiouny and H. Martin* (4) which studies flow distribution in the channels between the heat exchanger plates and the total pressure drop for "U" and "Z" configurations. Since the study did not consider friction, problems raised in following investigations, when experimental results showed that there was a pressure rise after branching (2). This phenomenon was later explained by *J. Wang*, whom also found solutions for both "U" (5) and "Z" (6) arrangements taking friction and inert effects into consideration.

It is a key to predict the performance and efficiency of manifold configurations so that high efficiency and cost reduction can be achieved through an optimal geometrical configuration of the solar collector (2).

For that reason, the following project studies the transient numerical analysis of the effect of non- uniform distribution of flow in an instantaneous system formed by a number of flat plate solar collectors and a heat exchanger using an implicit finite difference method in an iterative scheme employing the MATLAB software.

1.1 Aim of the work

The purpose of this work is the analysis by numerical means, the effect that the non- uniform distribution of water flow has in a parallel system of flat plate solar collectors.

The numerical model consists of a differential balance of energy for both; solar collectors and the auxiliary heat exchanger. The equations for the energy balance in the solar collector is based on the model presented by Ahmad M. Saleh, *"Modeling of flat- plate solar collector operation in transient state"* (7). The flow distribution will be estimated with the Bassiouny model (4).

As the experimental project could not be developed due to the difficulties of testing a solar collector and the lack of one, the needed parameters for the study were obtained through an initial dimensioning of a hypothetical Hot Water Service system implemented in a chosen building.

The selected building is the residence hall "Fernando Abril Martorell" located in Leganés, Madrid (Spain). This building was elected because it is isolated, that is,

there aren't any structures or vegetation such as trees that would cause shades (and hence losses) at the roof, where the solar collectors will be placed.

The system was sized following the current regulations established in the "*Documento Básico (DB) HE"* of the *"Código Técnico de la Edificación" (CTE)* (8), which establishes the rules and necessary procedures to meet the basic requirements for energy saving.

1.2 Work structure

This project is divided into 8 different chapters whose contents are described below.

Chapter 1, INTRODUCTION, presents the importance of the research and development of flow distribution in manifolds due to its numerous applications in science and technology. It also includes the aim of the work and this work structure.

Chapter 2, SOLAR WATER HEATING SYSTEMS, encloses general concepts regarding solar energy and a more in detail study of solar thermal energy including one of its main applications, that is, Hot Water Service (HWS). It additionally explains the types and components of a HWS system because of its relevance to this work.

Chapter 3, SOLAR COLLECTORS, contains a general introduction of the types and applications of solar collectors and a fully study of flat plate solar collectors including its components.

In Chapter 4, CALCULATING THE DEMAND, the necessary heat to satisfy the demand and corresponding flow of consumption for the instantaneous HWS system proposed for this project is dimensioned following the current regulations established in the *"Código Técnico de la Edificación (CTE)- DBHE"* for energy saving.

Chapter 5, CALCULATION OF LOSSES, includes the calculation of losses due to orientation, inclination and shades explaining all the considerations taken into account and following the criteria stated in *CTE- DBHE*.

In Chapter 6, DIMENSIONING THE SOLAR COLLECTOR, the necessary parameters for the numerical model such as the water flow in the solar collector, the inlet and outlet temperatures of the collector and the geometry of the collector, were found.

In Chapter 7, MATHEMATICAL FORMULATION, the development of the model based on Ahmad M. Saleh's thesis is fully explained, including the governing equations obtained from the energy balances in the components of the solar

collector (glass cover, air gap, absorber plate, insulation and working fluid) and the heat exchanger.

In Chapter 8, RESULTS AND CONCLUSION, the results acquired from the model using MATLAB (code included in Appendix A) are displayed using graphs and fully explained. Lastly, a conclusion is finally drawn from the obtained results.

2 SOLAR WATER HEATING SYSTEMS

2.1 Introduction to Solar energy

Solar energy is a renewable energy obtained from the sun (a powerful energy source), able to generate both heat and electricity (9). Although it is common to categorize this technology as "relatively new", solar energy has been around for thousands of years. In fact, its history spans from the 7th century B.C., when sun heat was concentrated through magnifying glasses to make fire, to today (10).

Depending on the technique used to collect the energy radiated from the sun, solar technology can be divided into three types (9):

- *Photovoltaic systems*: Which use photovoltaic solar panels to transform the sun's rays into electricity directly from sunlight.

- ***Solar Thermal energy***: It harnesses the sun's heat through solar collectors.

- *Solar electricity*: It transforms heat into electricity in an indirect manner with the help of concentrating solar collectors.

Spain is a particularly favored country in comparison to other European countries due to its privileged location and climatology, which is probably one of the main reasons, is the most experienced country regarding this technology. It has been considered the world's leader in the development and implementation of photovoltaic technology, as well as, ranking first in concentrating solar collector systems; technology which has also been exported to many countries (11).

Table 1 shows a number of benefits (12) and drawbacks associated to solar energy (13).

ADVANTAGES	DISADVANTAGES
Renewable energy source	*High initial cost*
Reduces electricity bills: some of the energy needs met with the implemented solar system	*Weather dependent*: Efficiency drops during cloudy and rainy days
Diverse applications (hot water service, space heating, electricity generation, etc)	*High solar energy storage cost* (batteries)
Low maintenance costs: The main maintenance cost is keeping the systems relatively clean (couple of times per year) since most reliable solar panel manufacturers give 20- 25 years warranty.	*Requires a lo*t of space
Technology development: Constantly advancing and improving	
Environmentally friendly: it does not pollute nor produce greenhouse gases	

2.2 Solar thermal energy systems

Nowadays, solar thermal energy is becoming an important renewable energy source; therefore the use of solar collectors is attractive, because of their simplicity and flexibility. Moreover, their attractiveness has grown in the last year due to the substantial decrease of their market place.

Solar thermal energy is present in a vast numbers of applications such as the simple heating of water service or heating of buildings, which are both mainly used in households and sometimes installed simultaneously (combined systems); solar thermal systems for cooling and heat- process production (14), or heating pools, only to mention a few.

Figure 2.1. Example of a combined system

Although, smaller installations such as households are already standardized, large systems show still a low standardization level, leading generally to the individual design and execution of each one (14). In years to come, further research in this field of solar thermal systems for cooling and heat- process production is required in order to improve energy efficiency and henceforward accelerate the integration of renewable energy technologies with buildings.

The main component of these systems is the solar collector, which can be classified according to its operating temperature with respect to the ambient air as follows:

- *Low temperature collectors*: They provide useful heat at temperatures close to the ambient temperature to avoid heat loss to the surroundings. The problem is that once the temperature rises, there is nothing to keep the harvested solar heat within the system, escaping thus to the surroundings (see Figure 2.2). They are used for pool heating. (12)

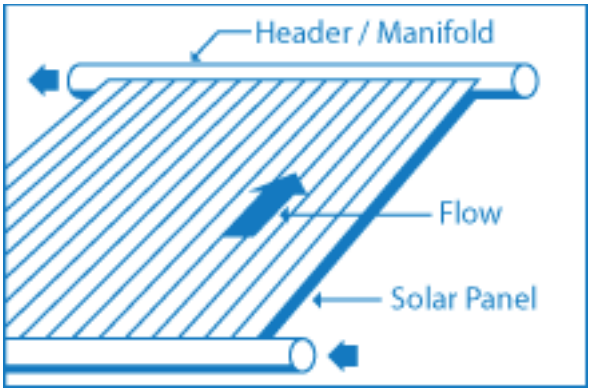

Figure 2.2 Example of a low temperature collector (12)

- ***Medium temperature collectors***: These collectors operate customarily between 30 and 300 °C above the ambient temperature. Some of their uses include HWS (up to 60°C) or space heating, where temperatures below 95°C are sufficient using flat plate solar collectors and temperatures of 100-220°C can be reached with evacuated tube collectors.

- *High temperature collectors*: These devices concentrate solar radiation to deliver useful heat at higher temperatures than 300 °C and are used for electric power generation in photovoltaic systems (15).

A simplified version of solar water heating systems is an installation made of two independent circuits:

a) *Primary circuit:* This circuit carries the working fluid (with a antifreeze solution for winter or cold weathers), which passes through the solar collectors, where it is heated by solar energy increasing its temperature, to finally transfer this heat in a heat exchanger to the second circuit.

b) *Secondary or process circuit:* The process of interest occurs in this circuit, which in this project consists of the HWS system.

With this architectures both fluids are never mix (16).

Also, these systems can be divided into active or passive systems depending on the circulation of the working fluid. *Passive* systems, also known as *drain down* systems, rely on gravity and the principle of "natural convection", where the water flows accordingly as it is heated; while *active* systems (or *recirculating* systems) use pumps to move the liquid. The latter are more efficient but involve a higher cost (17).

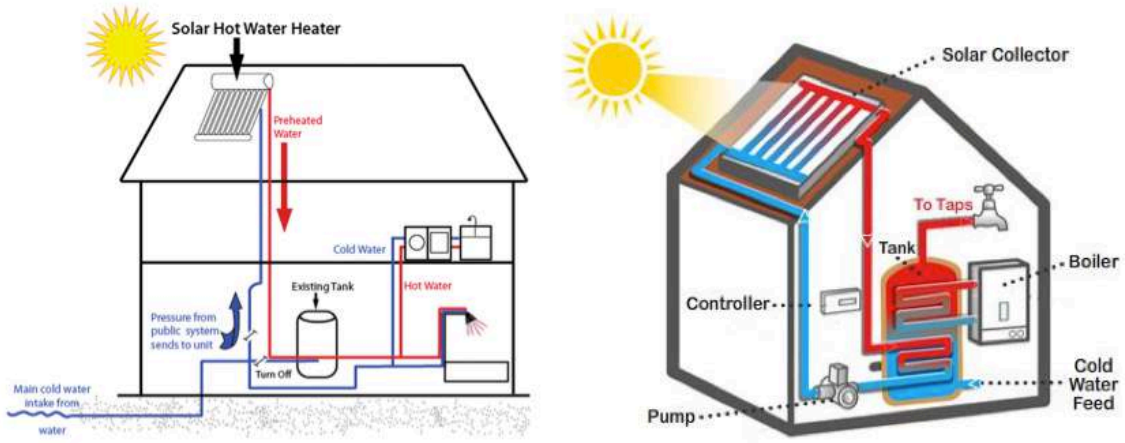

Figure 2.3. Passive system (left) vs Active system (right)

Hot Water Service (HWS) is one of the most extended practices of solar energy even though it is not necessarily the easiest to apply neither the most profitable. These systems are designed to cover the HWS necessities throughout the whole year taking into account the fewer amount of solar radiation during winter. They can be implemented by themselves or with an auxiliary conventional system (boiler) (18).

The hot water obtained from the HWS installation is used for sanitary purposes such as toilets, showers, etc., as well as other cleaning uses (washing machine, dishwasher, scrubbing dishes or floors…); hence, these systems are great for households, hotels, restaurants, hospitals, residence halls, and any type of building where hot water is needed on a daily basis (16).

2.3 Types of Hot Water Service (HWS) systems

There are two types of systems that can be distinguished depending on the production of HWS.

2.3.1 Instantaneous production

The main feature of this type of installation is that the water is consumed as it is produced as there is a continuous flow of hot water; hence the heat exchangers are design satisfying the maximum demand of the building (18). The temperature can be managed through controls that allow the user to set the most suitable temperature, thus saving energy and avoiding undesirable burns (19).

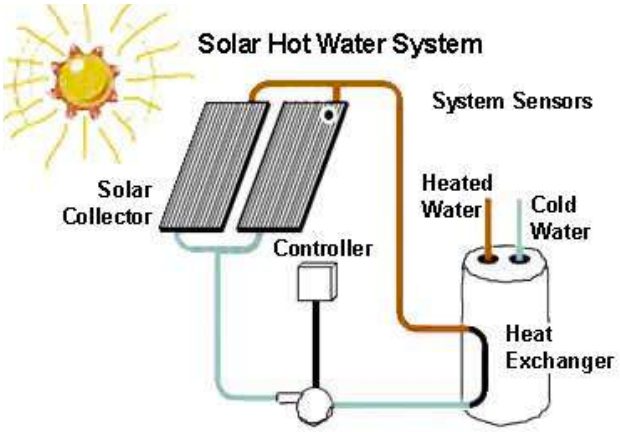

Figure 2.4. Example of an instantaneous HWS system

2.3.2 Production with accumulation

This type of systems store the hot water in tanks until it is ready to be used helping to reduce the power for production. Depending on the volume of accretion, they can be separated into *accumulation* and *semi- accumulation* systems (18).

The essential component is the tank, which can be either basic or incorporate a heat exchanger in its inside.

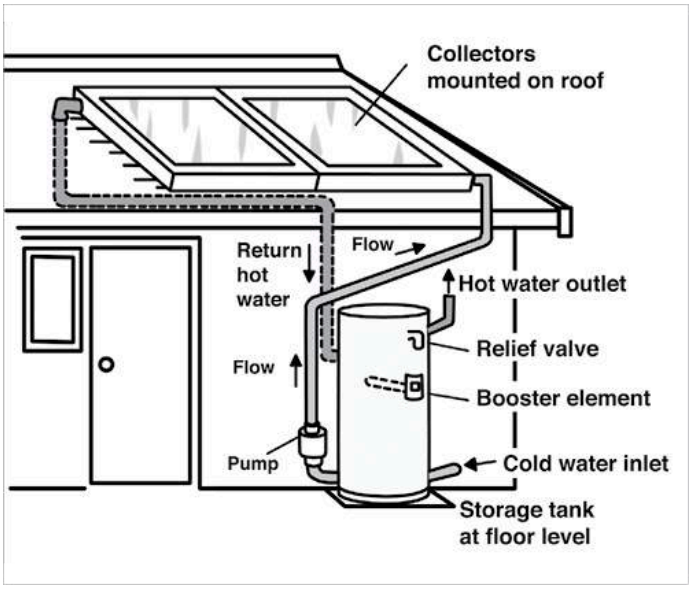

Figure 2.5. Example of a HWS system with accumulation (19)

2.4 Components of an active HWS system

The main components found on a low temperature solar water heating system are:

- *Solar collectors*: This device is the key component of the system as it converts the incoming solar radiation into heat in order to transfer this heat to a fluid flowing through the collector (20). This component will be explained in detail in the next chapter, as it is required for the correct understanding of this thesis. (Further explained in section 3)

- *Heat exchangers*: Are devices that transfer thermal energy (enthalpy) from one group of fluids to another group. For the system studied they are used to transfer the energy from the solar collector circuit to the HWS circuit. They can be made of several materials such as steel, copper, bronze, stainless steel, aluminum or cast iron. Solar heating systems usually employ copper because of its properties, like good thermal conductor and resistance to corrosion (17).

- *Heat transfer fluids*: They carry heat through the solar collector to the heat exchanger (in instantaneous systems) or to the storage tank (in case of an accumulation system). The criteria considered to select the fluid are: coefficient of expansion, viscosity, thermal capacity, freezing, boiling and flash points (17). The most frequently fluids are:
  - Air
  - Water
  - Glycol- water mixtures, especially useful in cold weathers because of their low freezing point
  - Refrigerants- phase change fluids (PCM)

- *Circulating pumps*: Solar water heating systems commonly use centrifugal pumps as they have both low power consumption and low maintenance, and flexibility. The material used for the pump depends on whether the system is closed or open loop, and working temperatures. Additionally, the overall pressure that it must create depends on the height the water must be lifted and the frictional resistance of the pipe system and other pressure losses, such as valves, turning, etc (17).

- *Storage tanks*: Integrated into accumulation systems. Their task is to hold water heated by the solar water heating system. More than one storage tank can be added to the system depending on the building's requirements.

- *Circulation system:* It is made of tubes covered with thermal insulation and other accessories mentioned below, which carry the fluids (16).

- *Others:* Sensors and controls, a check valve that permits the fluid to flow in one direction only, pressure relief valve to prevent high temperatures in the system, pressure and temperature gauges, etc (17).

3 SOLAR COLLECTORS

3.1 Introduction

A solar thermal collector is a special kind of heat exchanger that enables the transformation of solar radiation energy into internal energy of the transport medium (20).

The solar energy collected in the solar collector is carried from the circulating fluid either directly to the equipment or to a thermal storage tank for later use (20). This may be achieved directly or through a heat exchanger.

There are two types of solar collectors:

- *Concentrating*: The interceptor is bigger than the absorber.

Figure 3.1. Examples of concentrating solar collectors

- *Non- concentrating*: The whole solar panel absorbs light since the collector area is the same as the absorber area.

For domestic and industrial water and/ or space heating purposes the non-concentrating solar collectors can be classified as:

- ***Flat plate solar collectors***
- *Evacuated tube solar collectors*

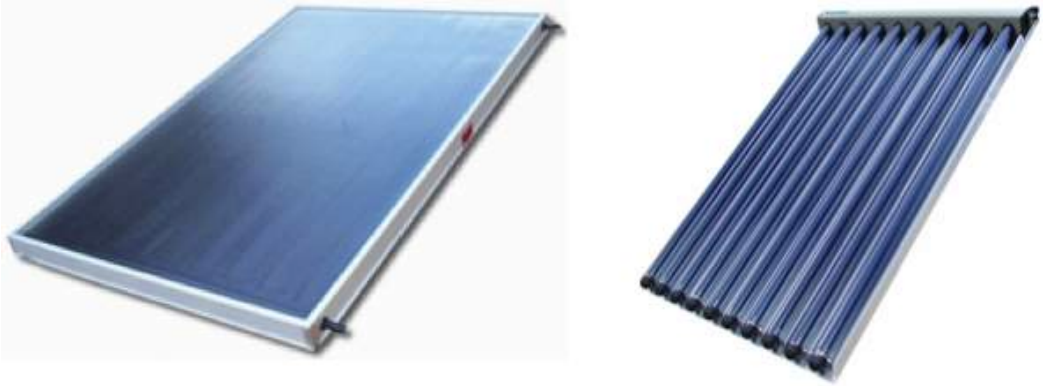

Figure 3.2. Types of non- concentrating solar collectors: Flat plate solar collector (left) and evacuated tube solar collector (right)

For the purpose of this project flat plate solar collectors will be further studied.

3.2 Flat plate solar collectors

Flat plate solar collectors, developed by Hottel and Whillier in the 1950s, are the most common type; being broadly used for domestic household hot water and space heating, where the temperature demanded is low (20).

They are generally fairly inexpensive in comparison with evacuated solar thermal collectors even though its reliance depends considerably on the variation of materials price that are used for its production (21).

The collectors can achieve up to 75% efficiency under perfect operating conditions, where the temperature of the inlet fluid is same or less than the ambient air temperature. However, perfect conditions are usually extremely rare. Moreover, it is important to take into consideration the position of the solar panel locating it as directly towards the sun as possible in order to maximize its efficiency (21). Plus, they only operate at maximum efficiency when the sunrays strike perpendicular to the flat plate.

3.3 Components of a flat plate solar collector

A flat plate collector compromises a series of vertical flow tubes (or risers) joined at the top and bottom to two larger diameter, horizontal pipes known as headers; all of which is enclosed in an insulated rectangular box covered with a translucent panel called glazing (22).

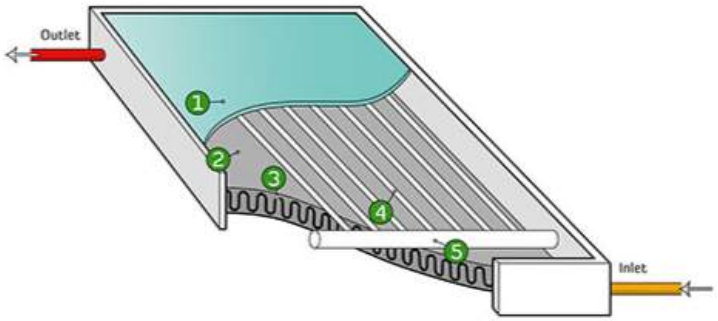

1. Glazing
2. Absorber plate
3. Insulation
4. Flow tubes or risers
5. Header

Figure 3.3. Components of a flat plate solar collector (21)

3.3.1 Glazing

The glazing is a transparent or translucent cover sheet, which shelters the flat plate solar collector. It is made out of glass or plastic, being the transmittance a key factor in the selection of the material.

The main function of the glazing is to diminish convective heat losses, that is, reduce heat radiation from the absorber into the environment using a similar method to a greenhouse.

The number of cover sheets may vary from none to three or more depending on the user's requirements (23).

3.3.2 Absorber plate

The absorber plate is the main element of a flat plate solar collector. It covers the full aperture area of the collector and is usually made out of metals materials such as copper, steel, stainless steel or aluminum (23).

The purpose of the absorber is to take up the maximum possible amount of solar irradiance to conduct heat into the working fluid with a smallest temperature difference in order to avoid the loss of heat to the surroundings as a function of the emittance of the surface. Thus, the metal material selected must have both high thermal conductivity and high absorptance. The absorber plate is usually black since dark surfaces display a higher degree of sunlight absorption (23). In fact, flat black paint has an absorptance of about 95% for incident shortwave radiation. Plus, it is durable and easy to apply (20).

To maximize the useful heat captured by a solar collector and reduce energy losses from radiation, absorbers usually have a selective surface coating, which is able to provide above 90% absorption. The coating allows the conversion of a high fraction of solar radiation into heat as well as simultaneously reducing the re-emission of heat.

Selective surfaces have a high absorptivity for short wavelength (visible) light and low to average absorptivity for long wavelength (thermal or infra- red) radiation; resulting in the surface ability to absorb solar energy successfully without re-radiating a high amount of thermal energy. Some frequently used coatings include black chrome, black nickel and aluminum oxide with nickel (23). Also, a relatively new type of coating applied via steam in a vacuum process is a titanium- nitride-oxide layer, which stands out for being both emission- free (quite low emission rates) and energy efficient (24).

There are several types of absorbers categorized according to the internal tubing designs, some of which include (25):

- *Harp*
  It involves a traditional design with bottom pipe risers and top collection pipe. It is used in low-pressure thermosyphon and pumped systems.

- *Flooded absorber* consisting of two sheets of metal stamped to produce a circulation flow ("Trickle type" of corrugated sheet).

- *Serpatine*
  The fluid passes only through one tube arranged in an "S" configuration. It maximizes temperature but not total energy yield in variable flow systems. It is used only in compact domestic hot water systems. Although, it can be easily fabricated and enables the parallel connection of several collectors, this configuration leads to a greater pressure loss than others like for example, parallel tubes.

- ***Parallel tube***
  It consists of a number of tubes known as rises placed vertically, which are connected to two horizontal pipes at their ends (headers). This is the type of absorber chosen for this project due to its higher efficiency in comparison to other configurations in consequence of its extended used of absorber fins. It also deals with lower pressure losses and temperature differences, hence contributing to its efficiency rate.

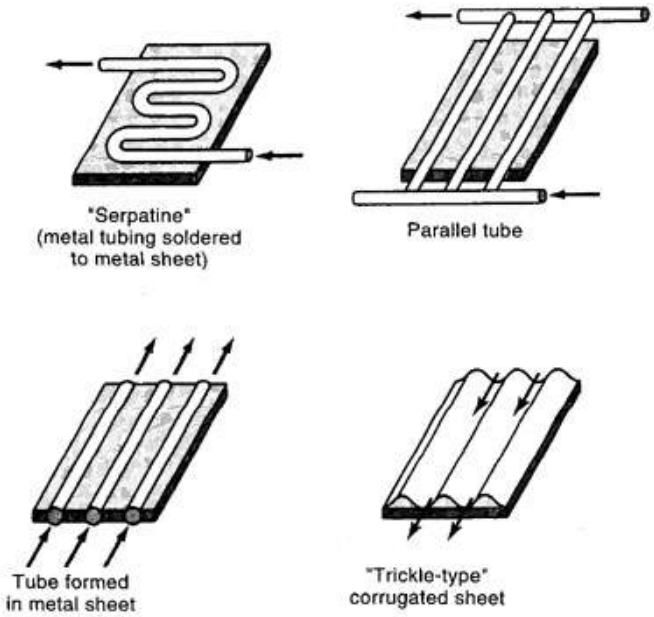

Figure 3.4. Types of absorbers according to internal tubing arrangement (25)

3.3.3 Insulation

With the intention of reducing conduction losses, both the sides and back surface of the absorber should integrate good insulation; which should be thick enough to make this kind of heat loss trivial.

Materials such as urethane or polyisocyanurate insulation are well suited, as they not only exhibit higher insulation value per centimeter of thickness than others do, but are additionally very easy to handle (23).

3.3.4 Enclosure

The enclosure is the collector housing containing all the elements; hence, the materials used must be robust and well protected by paint. Moreover, it must provide suitable anchorage points so it can be possible to secure the solar collector to the exterior of the building.

The main purposes of the enclosure are to protect the absorber from the weather, to secure the complete solar collector and last but not least, to reduce back and side heat losses; thus, the necessity to insulate the case (23).

3.3.5 Flow tubes

The flow tubes are in charge of taking the hot fluid from the solar collector to the household or storage tank. These pipes are usually made out of copper and in some cases plastic, although it is not highly recommended due to the risk of the relief valve failing.

The separation of the tubes varies according to cost and efficiency. Closed spaced tubes lead to a higher cost but improve the efficiency (23).

4 CALCULATING THE DEMAND

Due its simplicity, for this project, an instantaneous HWS system was chosen to dimension the solar collectors geometry. Other considerations and assumptions will be further explained in the sections below, following the relevant steps stated in the corresponding regulations.

4.1 Location

The flat plate solar collectors will be placed in the Residence hall *Fernando Abril Martorell* located in Leganés (Madrid, Spain) with latitude of $40° 19' N$. The complete capacity of the building is of 310 people, which is the amount that will be considered for the dimensioning.

Figure 4.1. Geographic placement of the building (26)

The residence hall is "isolated", therefore, no obstacles such as other higher buildings or trees, which could block the sunlight creating shades in the solar collectors. Thus, the solar collectors will be positioned at the roof of the building.

Figure 4.2. Residence hall "Fernando Abril Martorell"

4.2 Initial data

To correctly estimate the necessary dimensions for the solar collector, it is necessary to obtain some previous data relevant for the calculations.

4.2.1 Mean temperature of network water

The following table contains the mean daily temperature of network water (°C) of the capital of Madrid (Spain) according to *Appendix B of DB- HE 4* (8).

JAN	FEB	MAR	APR	MAY	JUN	JUL	AUG	SEP	OCT	NOV	DEC	ANNUAL AVERAGE
8	8	10	12	14	17	20	19	17	13	10	8	13

Table 4.1. Mean daily temperature (°C) of network water in Madrid

Even though the location of the building is not exactly in the capital but rather in the suburbs of Madrid, due to the insignificant difference between the latitudes of Leganés and Madrid, the data shown in Table 4.1 will not be readjusted.

4.2.2 Average daily temperature and optimum tilt angle

The following table shows the optimum tilt angle of the solar collector, β_{OPT}, the solar irradiance for both; a perpendicular plane (direct), and a plane with the optimum tilt angle (H_{OPT}), and the average daily ambient temperature, T_a, for the residence hall. This data was provided by the *geographic information system* from the *European's Commission Joint Research Centre (JRC)* (27).

	β_{OPT} (°)	IRRADIANCE $\left(Wh/m^2 \cdot day\right)$		T_a (°C)
		Q''_{OPT}	DIRECT	
JANUARY	64	3600	3300	4.1
FEBRUARY	56	4750	4380	5.3
MARCH	43	5930	5200	8.9
APRIL	27	6020	5550	11.5
MAY	15	6410	6520	16.1
JUNE	7	7000	7960	22.2
JULY	10	7480	9270	25.1
AUGUST	23	7300	8080	24.7
SEPTEMBER	39	6520	6520	20.2
OCTOBER	52	5310	4850	13.9
NOVEMBER	61	3980	3580	8.1
DECEMBER	66	3490	3230	4.5
MEAN	36	5650	5710	13.7

Table 4.2. Optimum tilt, irradiance and average daily temperature in Madrid

4.2.3 Solar Radiation

Solar Radiation is defined as the amount of electromagnetic energy emitted by the Sun, or, in other words, the power per unit area received from the Sun (28).

The intensity of the solar irradiance depends, amongst other factors, on the solar height, that is, the trajectory of the sunrays inside the atmosphere, and the latitude of the place of interest.

Figure 4.3 below shows the different irradiance levels for Madrid according to the *"Solar Radiation Atlas in Spain"* (29), which quantifies and presents graphically this data collected since 1983 to 2005 with sufficient spatial resolution.

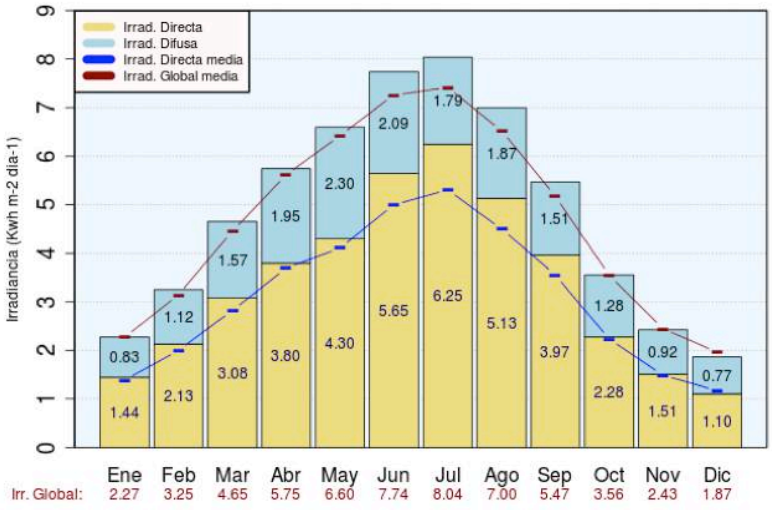

Figure 4.3. Different types of solar radiation levels in Madrid

Table 3 shows the average monthly and annual irradiance that reaches the Earth's surface in Madrid according to Figure 10 shown above.

	IRRADIANCE $\left(kWh/m^2 \cdot day\right)$	
	GLOBAL	DIRECT
JANUARY	2.27	1.44
FEBRUARY	3.25	2.13
MARCH	4.65	3.08
APRIL	5.75	3.80
MAY	6.60	4.30
JUNE	7.74	5.65
JULY	8.04	6.25
AUGUST	7.00	5.13
SEPTEMBER	5.47	3.97
OCTOBER	3.56	2.28
NOVEMBER	2.43	1.51
DECEMBER	1.87	1.10
MEAN	4.88	3.39

Table 4.3. Average value for Global and Direct Solar Irradiance in Madrid

4.3 Demand of HWS

First of all, the demand of HWS must be obtained. Table 4.1 of the *DBHE* shows the reference demand values for a temperature of 60°C depending on the utilization of the space, being in this case a residence hall. The following table includes the unitary demand stated on the *DBHE* (8).

Demand criteria	$l/_{day \cdot unit}$	Unit
Residence Hall	41	Per person

Table 4.4. Reference demand for a temperature of 60℃

In this case, the temperature at which HWS is supplied has been set to **45**°C in regards of the needs of consumption. Therefore, following the corresponding procedure established by the regulations present in the *DBHE*, the demand will be adjusted accordingly:

$$D(T) = \sum_{1}^{12} D_i(T) \quad (1)$$

$$D_i(T) = D_i(60℃) \times \left(\frac{60 - T_i}{T - T_i}\right) \quad (2)$$

Where,

$D(T)$: Demand of HWS at temperature T
$D_i(T)$: Demand of HWS for month "i" at temperature T
$D_i(60℃)$: Demand of HWS for month "i" at 60°C
T: Final temperature (45°C in this case)
T_i: Mean minimum temperature of network water

As not all the residents will be demanding water at the same time, a centralization factor of 75% was taken into account as the *DBHE* specifies in the following table:

No. of students	$N \leq 1$	$4 \leq N \leq 10$	$11 \leq N \leq 20$	$21 \leq N \leq 50$	$51 \leq N \leq 75$	$76 \leq N \leq 100$	$N \geq 101$
Centralization factor	1	0.95	0.90	0.85	0.80	0.75	0.70

Table 4.5. Value of centralization factor (8)

It is important to mention the fact that during the months of summer the residence hall will have a much lower occupation because the students are on their summer

break. Thus, an estimated occupation of 60% for June and 40% for July and August has been considered.

MONTH	NETWORK'S TEMP. OF MADRID (°C)	DAILY DEMAND $(l/day \cdot person)$	OCCUPATION	MONTHLY DEMAND $(l/month)$	NO. OF DAYS OF THE MONTH	TOTAL (l)
January	8	57,62	217	12503,89	31	387620,64
February	8	57,62	217	12503,89	28	350108,97
March	10	58.57	217	12710	31	394010
April	12	59.64	217	12941,09	30	388232,72
May	14	60.84	217	13202	31	409262
June	17	62.96	186	11711,35	30	351340,71
July	20	65.60	124	8134,4	31	252166,4
August	19	64.65	124	8017,07	31	248529,38
September	17	62.96	217	13663,25	30	409897,5
October	13	60.22	217	13067,46	31	405091,53
November	10	58.57	217	12710	30	381300
December	8	57.62	217	12503,89	31	387620,64
					TOTAL	**4365180,53**

Table 4.6. Calculating the demand of HWS at temperature of 45℃

Finally, the average daily demand of HWS at temperature $T = 45$°C is:

$$D(45°C) = \frac{4365180{,}53\ l/year}{365\ days} = 11959.40\ {}^{l}/_{day}$$

$$\boxed{D(45°C) = 11959.40\ {}^{l}/_{day}}$$

4.4 Annual average flow of consumption

The daily demand of HWS has been calculated, the necessary flow of water for consumption can be estimated taking into consideration the approximate number of hours of sun per day shown in Table 4.6, that is, the amount of time that the system is working.

	HOURS OF SUN	
	TOTAL $(^{h}/_{month})$	DAILY $(^{h}/_{day})$
JANUARY	140	4.52
FEBRUARY	164	5.86
MARCH	221	7.13
APRIL	219	7.30
MAY	256	8.26
JUNE	299	9.97
JULY	344	11.10
AUGUST	328	10.58
SEPTEMBER	252	8.40
OCTOBER	198	6.39
NOVEMBER	155	5.17
DECEMBER	115	3.71
ANNUAL AVERAGE	224.25	7.36

Table 4.7. Number of hours of sun in Madrid (30)

Consequently, the annual average flow of consumption, $\dot{m}_c$, would be:

$$\dot{m}_c = \frac{11959.40\ {}^{l}/_{day} \cdot 1\ {}^{kg}/_{l}}{7.36\ {}^{h}/_{day} \cdot 3600\ {}^{s}/_{h}} = 0.451\ {}^{kg}/_{s}$$

$$\boldsymbol{\dot{m}_c = 0.451\ {}^{kg}/_{s}}$$

4.5 Minimum solar contribution

The annual minimum solar contribution is defined as the fraction between annual solar values required for the system to function and annual daily demand of HWS obtained from the monthly average values.

To find out the minimum solar contribution required for the system, the climate zone for Leganés must first be determined. The following table shows the different irradiance levels, measured both in MJ/m^2 and kWh/m^2, which divide Spain into five different climate zones (8).

Climate zone	MJ/m^2	kWh/m^2
I	$H < 13.7$	$H < 3.8$
II	$13.7 \leq H < 15.1$	$3.8 \leq H < 4.2$
III	$15.1 \leq H < 16.6$	$4.2 \leq H < 4.6$
IV	$16.6 \leq H < 18.0$	$4.6 \leq H < 5.0$
V	$H \geq 18.0$	$H \geq 5.0$

Table 4.8. Annual average global solar radiation (8)

Taking into account the global solar radiation found in section 4.2.3, it can be seen that the value is comprehended between the values $4.6 \leq H < 5.0$, making the location of the residence hall part of ***climate zone IV***.

Building's total demand of HWS $litres/day$	**Climate zone**				
	I	II	III	IV	V
50 – 5,000	30	30	40	50	60
5,000 – 10,000	30	40	50	60	70
> 10,000	30	50	60	70	70

Table 4.9. Minimum annual solar contribution for HWS in % (8)

Considering the total daily demand of HWS calculated in section 4.3 and the requirements stated in Table 4.9 (*DBHE)*, the minimum solar contribution for this case can be obtained.

Total daily demand of ACS for the residence hall $(\boldsymbol{l/day})$	**Climate zone**
$\mathbf{11959.40}$ (> 10,000)	IV
Minimum solar contribution of $\boldsymbol{f = 70\%}$	

Table 4.10. Minimum solar contribution, f, of the HWS system

4.6 Thermal energy demand

The minimum thermal energy demand or heat required to satisfy the demand, can be calculated making an energy balance for the HWS circuit:

$$Q_{HWS} = \dot{m}_c \cdot c_p \cdot (T_{cons} - T_{net}) \quad (3)$$

Where,

Q_{HWS}: Heat transferred to the HWS (kW)
c_p: Specific heat of water $C_p = 4.18\ {}^{kJ}/_{kg°C}$
T_{cons}: Temperature of consumption (°C)
T_{net}: Mean minimum temperature of network water (°C)

The other parameters were obtained earlier and can be found in the following sections of this project:

- The water flow of consumption, $\dot{m}_c \Longrightarrow$ Section 4.4
- $T_{cons} \Longrightarrow$ Section 4.3
- $T_{net} \Longrightarrow$ Section 4.2.1

Thus,

$$Q_{HWS} = 0.451\ {}^{kg}/_{s} \cdot 4.18\ {}^{kJ}/_{kg°C} \cdot (45 - 13)°C$$

$$\boldsymbol{Q_{HWS} = 60.37\ kW}$$

Finally, considering the minimum solar contribution requirement established in the *DBHE* (Section 4.5) the system must provide the following minimum heat, Q_{min}, to be implemented:

$$Q_{min} = f \cdot Q_{HWS} \quad (4)$$

Where,

Q_{min}: Minimum heat provided by the HWS system

Therefore,

$$Q_{min} = 0.7 \cdot 60.37\ kW$$

$$\boxed{Q_{min} = 42.23\ kW}$$

5 CALCULATION OF LOSSES

5.1 Losses due to orientation and inclination

In accordance to *DBHE* (8) and *"Pliego de condiciones técnicas para instalaciones de baja temperatura"* (31) the losses due to orientation and inclination of the solar collector can be calculated as a function of the following parameters:

- Tilt angle, β, defined as the angle that the surface forms with the horizontal plane.

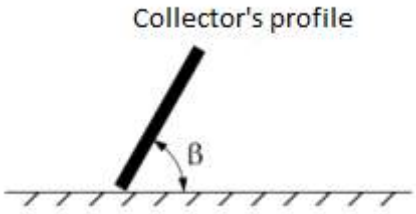

Figure 5.1. The tilt angle (8)

- Azimuth's angle, α, which is the compass direction from which the sunlight is arriving. Also defined as the array's east- west orientation in degrees (32).
  It determines the approximate amount of solar radiation (in hours) that the collector will receive. According to the *CTE DBHE 4* (8), the values considered are 0° when facing South, −90° for collectors facing East, and finally +90° for collectors facing West.

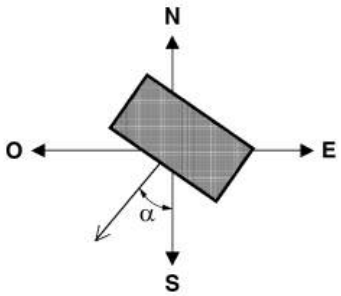

Figure 5.2. Representation of the azimuth's angle

The next figure shows a clearer understanding of both, the tilt and azimuth angle (in this case named as γ) of the solar collector:

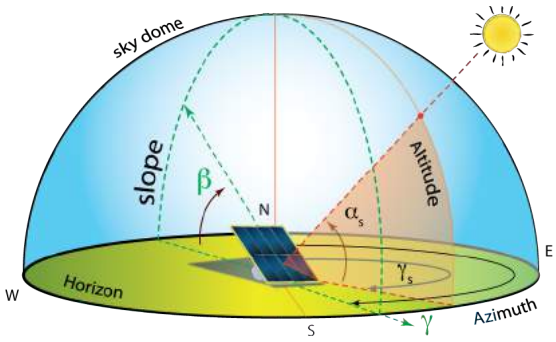

Figure 5.3. Collector- sun orientation (33)

In view of obtaining a higher efficiency, the following criteria (34) were followed:

- The collector will be facing **South** ($\alpha = 0°$) as it is the optimum orientation for a building located in the Northern Hemisphere.

- Although the optimum tilt according to the earlier studies of solar radiation is equal to 36°, this number will not be considered. Instead, an initial assumption of $\beta = 35°$ will be used in order to simplify the following calculations as it only differs in 1° making the disparity almost negligible.

Figure 5.4 describes a graphic method to obtain the range of possible tilt angles (β) for a latitude of $\phi = 41°$, satisfying the corresponding requirements established in the *CTE- DBHE* listed in Table 5.1 shown below. The method consists of a sphere divided in several portions by different patterns, where each pattern represents the energy percentage from the peak value due to orientation and tilt losses.

Case	Orientation and inclination	Shades	Total
General	10%	10%	15%

Table 5.1. Maximum admissible losses (8)

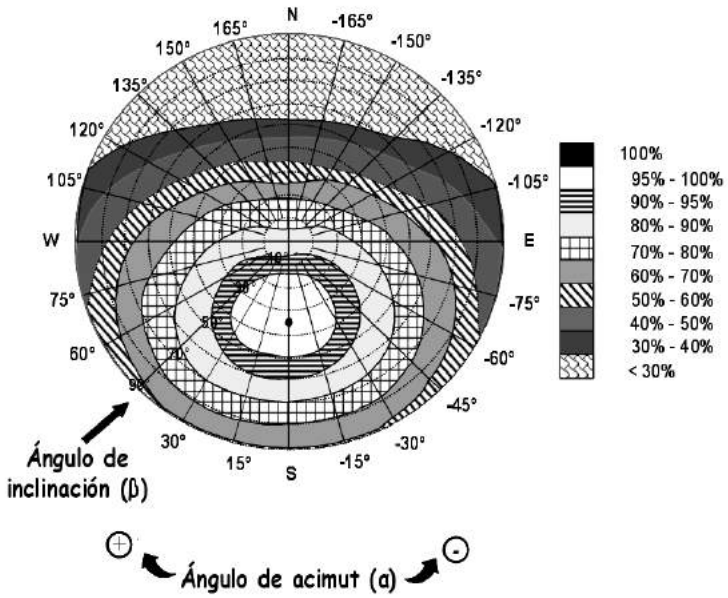

Figure 5.4. Graphic method to obtain the orientation and tilt losses

The yellow line in Figure 5.5 shows the azimuth line. Therefore, the intersection points of this line with the maximum admissible loss for the general case shown in Figure 5.1, that is, 10% of admissible losses (outer edge of the $90-95\%$ region in red), show the values of the maximum and minimum tilt.

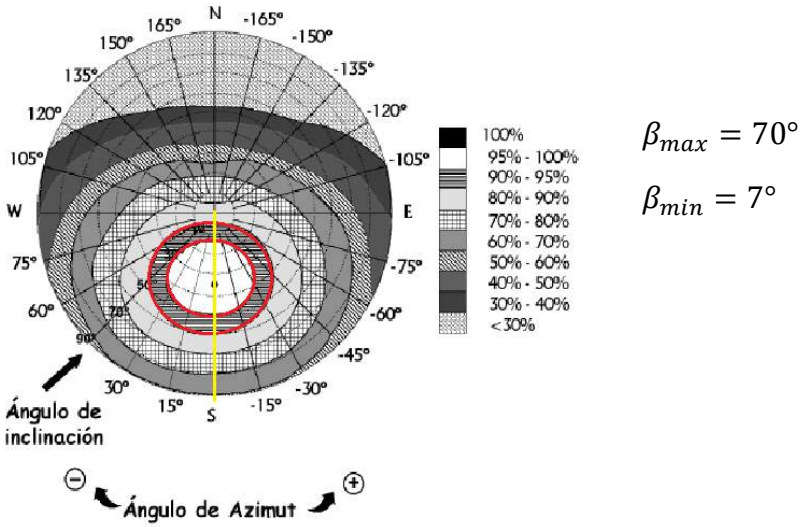

Figure 5.5. Representation of the maximum admissible losses (red) and the azimuth line (yellow)

The corrected limits for a building placed in Leganés with a corresponding latitude of $\phi = 40.2°$ are as follow:

- Maximum tilt:

$$\beta_{max} = \beta_{max}(\emptyset = 41°) - (41° - latitude) \quad (5)$$

$$\beta_{max} = 70° - (41° - 40.2°)$$

$$\boxed{\beta_{max} = 69.2°}$$

- Minimum tilt:

$$\beta_{min} = \beta_{min}(\phi = 41°) - (41° - latitude) \quad (6)$$

$$\beta_{min} = 7° - (41° - 40.2°)$$

$$\boxed{\beta_{min} = 6.2°}$$

Thus, the inclination of the collector value must be comprehended between these two values; and, in view of achieving a higher efficiency; the chosen tilt must intersect the azimuth line somewhere in the $95 - 100\%$ efficiency circle. Consequently, the chosen tilt was correctly estimated.

$$5.2° \leq \beta \leq 69.2° \rightarrow \beta = 35°$$

Finally, considering a preference demand during winter, we can obtain the optimum tilt angle:

$$\beta = 35° + 10°$$

$$\boxed{\boldsymbol{\beta = 45°}}$$

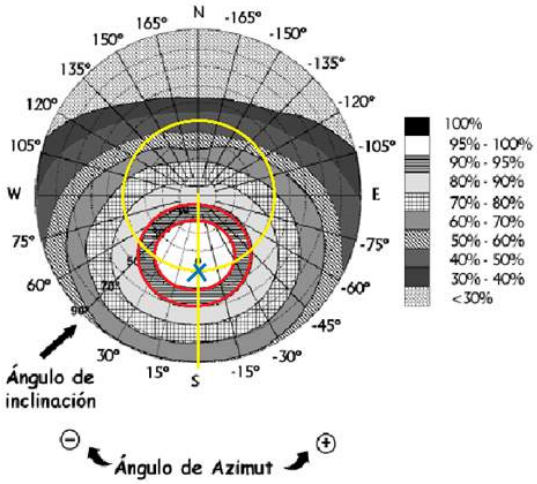

Figure 5.6. Final representation of the azimuth and tilt angles

Therefore, as it can be seen in the Figure 5.6 above, the intersection point (marked with a blue X) between the azimuth and the tilt lies in the $95 - 100\%$ region, leaving a maximum loss for solar radiation of less than 5%.

Finally, the Equation (6) obtained from the *DBHE* (8) is used as a tool to find an exact percentage of losses and verify the graphic result.

$$Losses\ (\%) = 100 \cdot [1.2 \cdot 10^{-4} \cdot (\beta - \beta_{OPT})^2 + 3.5 \cdot 10^{-5}\alpha^2] \quad for\ 15° < \beta < 90° \qquad (7)$$

$$Losses = 100 \cdot [1.2 \cdot 10^{-4} \cdot (35° - 36°)^2 + 3.5 \cdot 10^{-5}0^2]$$

$$\boxed{\boldsymbol{Losses = 0.012\ \%}}$$

5.2 Losses due to shades

The losses due to shades are expressed as the percentage of global solar radiation that would fall upon the mentioned surface if there were not any shade.

These losses could be due to the placement of the solar collectors or the proximity of other buildings, which could create shades during the day. In this case, there aren't any buildings nearby that could create these mentioned shades, and the solar collectors will be placed at the roof where the trees cannot create any shades either.

Furthermore, it will not be necessary to calculate the distance between the rows, as there will be only one row.

6 DIMENSIONING THE SOLAR COLLECTOR

6.1 The HWS system

To understand the procedure follow to dimension the solar collector, the HWS system's operation and features will be shortly explained below.

The system used to produce HWS is of instantaneous production divided into two separate circuits for better comprehension. Figure 6.1 shows a scheme of the system used with the corresponding components listed. The description of each component as well as its purpose was explained in section 2.4 of this document.

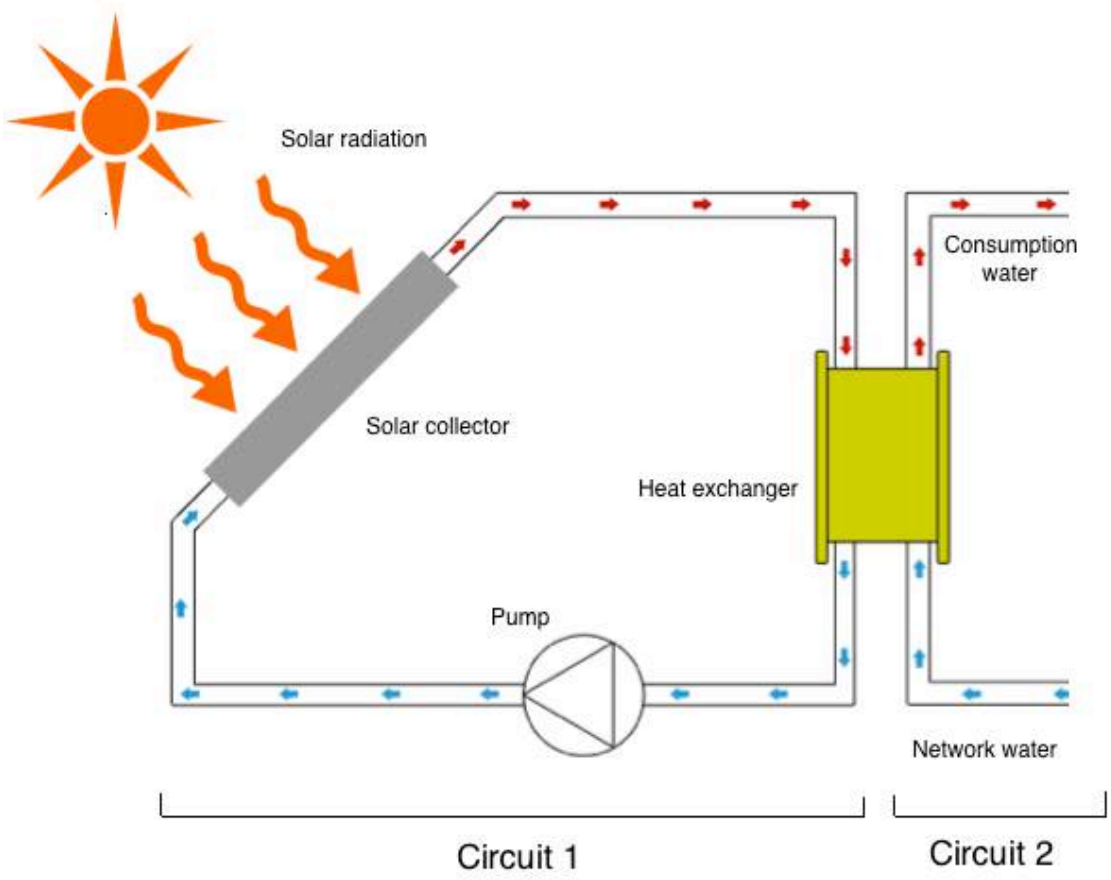

Figure 6.1. Scheme of the HWS system (35)

6.2 Water flow in the first circuit

The water flow in the solar collector, $\dot{m}_s$, can be obtained through an energy balance in Circuit 1:

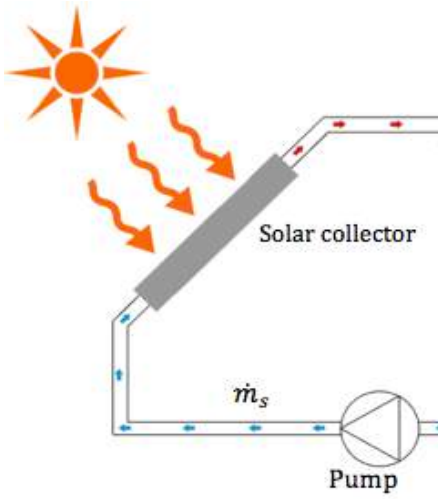

Figure 6.2. Exchange system (Circuit 1)

$$\dot{m}_s \, c_p \, \Delta T_s = \frac{1}{\eta} \cdot Q_{HWS} \qquad (8)$$

Where,

$\dot{m}_s$: Water flow in the first circuit (kg/s)
ΔT_s: Temperature difference in the solar collector (°C)
η: Efficiency of the solar collector

Assuming an efficiency of $\boldsymbol{\eta \approx 0.75}$ and a maximum temperature difference in the solar collector of $\boldsymbol{\Delta T_s \approx 5}$°C based on other working papers (36) and taking into consideration that there should not be a higher temperature difference due to the premature wear it could cause in the heat exchanger, the value of the water flow, $\dot{m}_s$, can be calculated clearing equation (8):

$$\dot{m}_s = \frac{Q_{HWS}}{\eta c_p \, \Delta T_s}$$

$$\dot{m}_s = \frac{60.37 \; kW}{0.75 \cdot 4.18 \; {}^{kJ}/_{kg°C} \cdot 5°C}$$

$$\boxed{\dot{m}_s = 3.85 \; {}^{kg}/_{s}}$$

6.3 Temperature difference in the solar collector

Although the temperature difference in the solar collector has been estimated in section 6.2, in order to obtain the water flow in the first circuit, a more accurate value for the average monthly inlet and outlet temperatures of the collector can be calculated through energy balances in the main components of the system and *the effectiveness- NTU method* explained in detail in *Chapter 11* of the book *"Fundamentals of Heat and Mass Transfer"* (37).

6.3.1 The effectiveness- NTU method

To define the effectiveness of a heat exchange, the maximum possible heat rate, q_{max}, must first be determined by the following general expression (37):

$$q_{max} = C_{min}(T_{h,i} - T_{c,i}) \quad (9)$$

Where,

C_{min}: Smallest heat capacity rate of either fluid in the heat exchanger; the hot fluid (C_h) or the cold fluid (C_c)
$(T_{h,i} - T_{c,i})$: The maximum temperature difference in the heat exchanger

On the other hand, the effectiveness of a heat exchanger, ε, is defined as the ratio between the actual heat transfer rate that the heat exchanger is providing taking into account the losses to the surroundings, q, and the maximum possible, q_{max} (37).

$$\varepsilon = \frac{q}{q_{max}} \quad (10)$$

Combining equations (8) and (9) a specific for or effectiveness- NTU (*Number of Transfer Units*) relation for any heat exchanger can be shown:

$$\varepsilon = f\left(NTU, \frac{C_{min}}{C_{max}}\right) = \frac{C_h(T_{h,i} - T_{h,o})}{C_{min}(T_{h,i} - T_{c,i})} = \frac{C_c(T_{c,o} - T_{c,i})}{C_{min}(T_{h,i} - T_{c,i})} \quad (11)$$

6.3.2 Obtaining the outlet temperature of the collector

To acquire the first equation (11) an energy balance in the heat exchanger can be made relating both circuits by stating that the necessary consumption in circuit 2 must be satisfy by the heat produced in circuit 1.

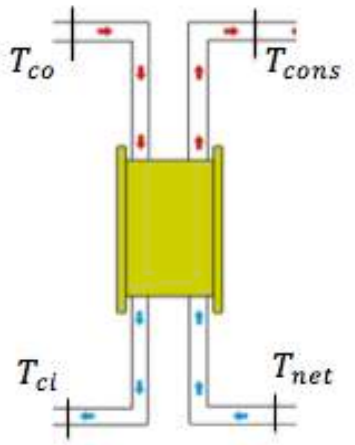

Figure 6.3. Energy balance in the heat exchanger

$$\dot{m}_s c_p (T_{co} - T_{ci}) = \dot{m}_c c_p (T_{cons} - T_{net}) \quad (12)$$

Where,

T_{co}: Outlet temperature of the solar collector
T_{ci}: Inlet temperature of the solar collector

Alternatively, a second equation can be determined using the NTU method explained in section 6.3.1 for which the effectiveness of the heat exchanger can be expressed as follows:

$$\varepsilon = \frac{T_{cons} - T_{net}}{T_{co} - T_{net}} \quad (13)$$

Finally, considering an efficiency of approximately $\varepsilon = 0.9$ and knowing the temperature of consumption, T_{cons}, and network water temperature, T_{net}, the temperature outside the collector, T_{co}, can be approximated from equation (12).

$$T_{co} = (T_{cons} - T_{net})\varepsilon + T_{net}$$

$$T_{co} = (45 - 13)°C \cdot 0.9 + 13°C$$

$$\boxed{\boldsymbol{T_{co} = 41.8\ °C}}$$

6.3.3 Obtaining the inlet temperature of the collector

As it was stated in Section 4.5 the minimum solar contribution is defined as the ratio between the total heat provided by the sun and the total heat used for the HWS system.

$$f = \frac{q_u}{Q_{HWS}} = \frac{\dot{m}_s c_p (T_{co} - T_{ci})}{\dot{m}_c c_p (T_{cons} - T_{net})} \quad (14)$$

Where,

Q_u: The useful heat rate provided by the sun

Consequently, clearing equation (14) and knowing the values of the other parameters as they have been calculated in the following sections of the work:

- $\dot{m}_s \Longrightarrow$ Section 6.2
- $\dot{m}_c \Longrightarrow$ Section 4.4
- $T_{co} \Longrightarrow$ Section 6.3.2
- $T_{cons} \Longrightarrow$ Section 4.3
- $T_{net} \Longrightarrow$ Section 4.2.1

The inlet temperature of the solar collector, T_{ci}, can be determined:

$$f = \frac{\dot{m}_s (T_{co} - T_{ci})}{\dot{m}_c (T_{cons} - T_{net})}$$

$$0.7 = \frac{3.85\ {}^{kg}/_{s}\ (41.8℃ - T_{ci})}{0.451\ {}^{kg}/_{s}\ (45 - 13)℃}$$

$$\boxed{\boldsymbol{T_{ci} = 39.17}\ ℃}$$

6.4 Geometry and useful heat of the series of solar collectors

A solar collector consists of a plate surface, which contains a material with high apsorptivity, with the addition of this material more solar radiation can be absorbed, increasing the collector's efficiency. This absorbed radiation is transfer to the working fluid that flows in array of tubes that are attached to the absorbed surface (See Figure 3.3). Therefore, estimating the heat absorbed by the flat plate, its geometry can be determined.

Since an initial estimated value for the required heat for the system has been previously found, Q_{HWS}, this new value must satisfy the following relationship:

$$A_{c,total}[Q'' - U_L(T_{pm} - T_a)] \geq Q_{HWS} \quad (15)$$

Where,

$A_{c,total}$: Total area of the solar collectors (m^2)
Q'': Global solar radiation $\left({}^{kWh}/_{m^2 \cdot day}\right)$
$U_L(T_{pm} - T_a)$: Heat losses at the walls of the collector
T_{pm}: Mean temperature of the collector (°C)
U_L: Total heat loss coefficient $\left({}^{W}/_{m^2°C}\right)$

T_a corresponds to the average ambient temperature shown in Table 4.2:

$$T_a = 13.7°C = 286.85K$$

Q'' must guarantee an efficient use of energy during the whole year. Thus, the mean global solar irradiance indicated in Table 4.8 will be used.

$$Q'' = 4.88\ {}^{kWh}/_{m^2 \cdot day}$$

The mean temperature of the collector, T_{pm}, can be easily calculated as the mean from the inlet temperature, T_{ci}, found in section 6.3.3 and outlet temperature of the collector, T_{co}, found in section 6.3.2.

$$T_{pm} = \frac{T_{ci} + T_{co}}{2} \quad (16)$$

$$T_{pm} = \frac{39.17°C + 41.8°C}{2}$$

$$T_{pm} = 40.48°C = 313.63K$$

The value of U_L can be approximated using the proposed equations by *V. K. Agarwal* and *D. C. Larson* (38), whom stated that the losses due to the bottom and edges of the collector can be neglected due to its little significance in comparison to the top surface losses. Moreover, the top surface losses, U_t, can be determined using the next equation derived from Klein (39), with an accuracy of $\pm 0.25\ {}^{W}/_{m^2°C}$ with respect to iterated values.

$$U_t = \left[\frac{N}{\left(\frac{C}{T_p}\right)\left(\frac{T_p - T_a}{N+f}\right)^{0.33} + \frac{1}{h_w}}\right]^{-1} + \frac{\sigma(T_{pm} + T_a)(T_p{}^2 + T_a{}^2)}{\left[\epsilon_p + 0.05N(1-\epsilon_p)\right]^{-1} + \left[\frac{2N + f' - 1}{\epsilon_g}\right] - N} \quad (17)$$

Where the dimensionless parameters f' and C are defined as follows,

$$f' = (1 - 0.04h_w + 0.005h_w{}^2)(1 + 0.091N)$$

$$C = 250[1 - 0.0044(\beta - 90)]$$

Being h_w (40):

$$h_w = 5.7 + 3.8v$$

Where,

U_t: Top loss coefficient $\left({}^{W}/_{m^2\text{°C}}\right)$
T_p: The plate's temperature
N: The number of transparent glass covers
σ: Stefan- Boltzmann constant $\left(5.67 \cdot 10^{-8}\, {}^{W}/_{m^2K^4}\right)$
h_w: Convective heat transfer coefficient due to wind $\left({}^{W}/_{m^2\text{°C}}\right)$
ϵ_p: Thermal emissivity of the absorbing plate surface
ϵ_g: Thermal emissivity of the cover (usually for glass= 0.88)
v: Wind's velocity $({}^{m}/_{s})$

Supposing a wind's velocity parameter of $v = 2\, {}^{m}/_{s}$ and the number of transparent glass covers $N = 1$;

$$h_w = 13.3\ {}^{W}/_{m^2\text{°C}} \longrightarrow f' = 1.147$$

For a tilt angle $\beta = 45$°C, the parameter C, which physically accounts for convective heat losses from the top of the absorbing plate as a function of the tilt angle, can be obtained:

$$C = 299.5$$

According to *Agarwal* and *Larson* (38) the plate's temperature can range from $T_p = 0 - 200$°C. Since HWS system function with medium temperature flat plate solar collectors, that is, temperatures lower than 95°C, the value will be assume to be approximately $T_p = 70$°C. Therefore, knowing the value of the rest of the parameters:

$$\boldsymbol{U_t = 4.75\ {}^{W}/_{m^2\text{°C}}}$$

Lastly, the total loss coefficient can be obtained adding all the heat losses (top, bottom and edges) which in this case will lead to $\boldsymbol{U_L = U_t}$ as the other two have been neglected (38).

Clearing Equation (15) the required collectors' area can be obtained:

$$A_{c,total} \geq \frac{Q_{HWS}}{[Q'' - U_L(T_{pm} - T_a)]} \quad (18)$$

Where, all the parameters have been already calculated in this section but Q_{HWS}, which can be found in section 4.6.

$$A_{c,total} \geq \frac{60.37 \cdot 10^3 Wh/day}{\left[4.88 \cdot 10^3 \ {}^{Wh}/_{m^2 \cdot day} - 4.75 \ {}^{W}/_{m^2 °C} (40.86 - 13.7)°C\right]}$$

$$\boxed{\boldsymbol{A_{c,total} \geq 12.71\ m^2}}$$

On the other hand, with the $A_{c,total}$ value found and a selected length, the total width of the connected solar collectors, W_{total}, can be calculated. Following the constructive criteria that the plates of the collector should not have any unions, this length must be equal or less than 2.5 m. In this case, the length will be of $\boldsymbol{L = 1.80\ m}$.

$$W_{total} = \frac{A_c}{L} \quad (19)$$

$$W_{total} = \frac{12.71\ m^2}{1.80\ m}$$

$$\boxed{W_{total} = 7.06\ m}$$

Hence, the number of solar collectors, N_c, needed for the system can be calculated:

$$W_{total} = N_c \cdot L \quad (20)$$

$$N_c = \frac{7.06\ m}{1.80\ m}$$

$$\boxed{\boldsymbol{N_c = 3.92 \approx 4}}$$

Therefore, the real width for one flat plate solar collectors, W_c, is:

$$W_c = \frac{W_{total}}{N_c} \quad (21)$$

$$\boldsymbol{W_c = 1.76\ m}$$

And thus, the area per collector:

$$A_c = W_c L \quad (22)$$

$$\boldsymbol{A_c = 3.17 m^2}$$

As the collectors are connected in parallel, they can function and be considered as one solar collector, thus, making an energy balance (39) in the collector we can obtain:

$$q_u = A_c N\left[Q'' - U_L\left(T_{pm} - T_a\right)\right] \quad (23)$$

Where,

q_u: Useful heat rate (kW)

Hence,

$$q_u = 3.17\ m^2 \cdot 4\left[4.88 \cdot 10^3\ {}^{Wh}/_{m^2 \cdot day} - 4.75\ {}^{W}/_{m^2 °C}\,(40.48 - 13.7)°C\right]$$

$$\boldsymbol{q_u = 60.26\ kW}$$

6.5 Geometry and useful heat of one solar collector

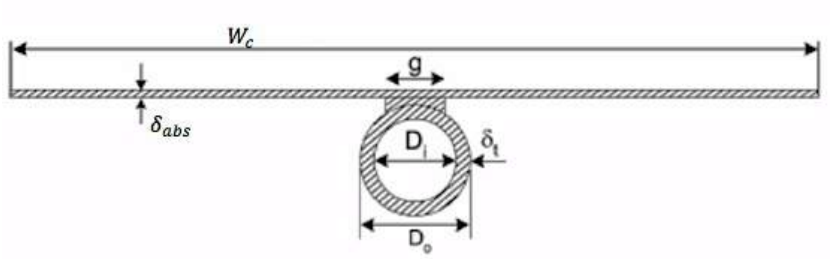

Figure 6.4. Geometry of the tube and fin of the absorber plate in a solar collector (40)

The separation between tubes shall be approximately between 10 to 15 cm since the greater the amount of tubes, the greater the pressure loss, and thus, the higher the unbalance, either for "Z" or "U" configuration types (4). Therefore, assuming a distance between tubes $d = 13\ cm$ and an internal diameter $D_i = 0.006\ m$, the number of tubes per collector, n, can be estimated. To obtain the number of tubes per collector, n, can be estimated.

$$W_c = n(D_i + d) \qquad (24)$$

$$n = \frac{1.76\ m}{(0.006 + 0.13)m}$$

$$\boldsymbol{n = 12.94 \approx 12\ tubes}$$

Finally, knowing that the solar collector has a number of tubes n, both the water flow per tube, $\dot{m}_i$, and the width per tube, W_i, can be calculated.

$$\dot{m}_i = \frac{\dot{m}_c}{n} \qquad (25)$$

$$\dot{m}_i = \frac{0.451\ {}^{kg}/_{s}}{12\ tubes}$$

$$\boldsymbol{\dot{m}_i = 0.0375\ {}^{kg}/_{s \cdot tube}}$$

$$W_i = \frac{W_{real}}{n} \qquad (26)$$

$$W_i = \frac{1.76\ m}{12\ tubes}$$

$$\boldsymbol{W_i = 0.147\ {}^{m}/_{tube}}$$

In contrast, the local efficiency factor of the collector (for design purposes), F', which represents the relationship of the thermal resistance between both the collector and the ambient, and the working fluid and the ambient (41), is given by:

$$F' = \frac{\frac{1}{U_L}}{W_c\left[\frac{1}{U_L[D_o + (W_c - D_o)F]} + \frac{1}{\pi D_i h_f} + \frac{1}{C_b}\right]} \quad (27)$$

Where,

D_o: Tubes outer diameter ($D_o = 7 \cdot 10^{-3} m$)

- h_f: Convective coefficient inside the tube

To calculate the convective coefficient, it is necessary to obtain first both, the Reynold's number, Re, and the Nusselt number, Nu. Consequently,

$$Re = \frac{\rho_w u L}{\mu} \quad (28)$$

Where,

ρ_w: The density of water $\left(1000\ {}^{kg}/_{m^3}\right)$
u: The velocity of water $({}^{m}/_{s})$
μ: The dynamic viscosity of water $(Pa \cdot s)$

For temperatures of approximately 70° (surface temperature of the absorber), the dynamic viscosity can be estimated to a given value of $\mu = 0.404\ Pa \cdot s$. Thus, estimating a velocity of water of $u = 1\ {}^{m}/_{s}$,

$$Re = \frac{1000\ {}^{kg}/_{m^3} \cdot 1\ {}^{m}/_{s} \cdot 1.80\ m}{0.404\ Pa \cdot s}$$

$$Re = 4.45 \cdot 10^3$$

Assuming that the Prandtl parameter for water is approximately $Pr = 10$, the surface heat flux will follow a turbulent flow (37). Hence,

$$Nu = 0.0308 Re^{4/5} Pr^{1/3} \qquad 0.6 \leq Pr \leq 60 \quad (29)$$

$$Nu = 55.03$$

Finally, supposing that the absorbers is made of copper, since it is a better conductor and less prone to corrosion than aluminum, and knowing that its thermal conductivity can be in between the values $k_{abs} = 372.1 - 385.2\ {}^{W}/_{mK}$, it can be assumed that $k_{abs} = 378.65\ {}^{W}/_{mK}$.

$$h_f = \frac{Nu \cdot k_{abs}}{D_i} \quad (30)$$

$$h_f = \frac{55.08 \cdot 378.65\ {}^{W}/_{mK}}{0.006\ m}$$

$$\boxed{h_f = 34760.07\ {}^{kW}/_{m^2K}}$$

- F: Fin's efficiency

This parameter can be calculated using the following expression (40):

$$F = \frac{\tanh\left(M \frac{W_i - g}{2}\right)}{M \frac{W_i - g}{2}} \quad (31)$$

Where,

g: Welding between the tube and the absorber plate

The dimensionless parameter M can be obtained as follows:

$$M = \left[\frac{U_L}{k_{abs} \cdot \delta_{abs}}\right]^{1/2} \quad (32)$$

Estimating the value of the thickness of the absorber's plate to $\delta_{abs} = 0.015\ m$ and being the rest of the parameters previously obtained (U_L found in section 6.4):

$$M = \left[\frac{4.75\ {}^{W}/_{m^2°C}}{378.65\ {}^{W}/_{mK} \cdot 0.015\ m}\right]^{1/2} = 0.914$$

And thus,

$$\boxed{F = 0.98}$$

- C_b: Conductance in the union between the tube and the plate

Supposing there is infinite conductance in the union between the tube and the plate:

$$C_b \to \infty \implies \frac{1}{C_b} = 0$$

Finally, substituting all the calculated parameters in equation (27):

$$\boxed{F = 0.96}$$

Now, a new energy balance equation can be used to find the useful heat transferred per tube, $Q_{u,i}$.

$$Q_{u,i} = W_i F' \left[Q'' - U_L \left(T_{pm} - T_a \right) \right] \quad (33)$$

$$Q_{u,i} = 0.147\, m \cdot 0.96 \left[4.88 \cdot 10^3 \ {}^{Wh}/_{m^2 \cdot day} - 4.75 \ {}^{W}/_{m^2 °C} \, (40.48 - 13.7)°C \right]$$

$$\boxed{\boldsymbol{Q_{u,i} = 670.71 \ {}^{W}/_{m}}}$$

Finally, it is necessary to check whether the value satisfies the following equation:

$$nLQ_{u,i} \geq \frac{q_u}{N_c} \quad (34)$$

Where,

$$nLQ_{u,i} = 14.49\ kW$$

$$\boldsymbol{\frac{q_u}{N} = 15.06\ kW}$$

It does not satisfy the criteria so the number of tubes is increased to $n = 13$;

$$\boldsymbol{nLQ_{u,i} = 15.69\ kW}$$

Therefore,

$$\boxed{nLQ_{u,i} \geq \frac{q_u}{N_c}}$$

7 MATHEMATICAL FORMULATION

The development of the mathematical model of the dimensioned flat plate solar collector is based on Ahmad M. Saleh's thesis (7), which describes a system considering its transient nature (39). The model fully describes the energy evolution of the glass cover, air gap, absorber, insulation and working fluid.

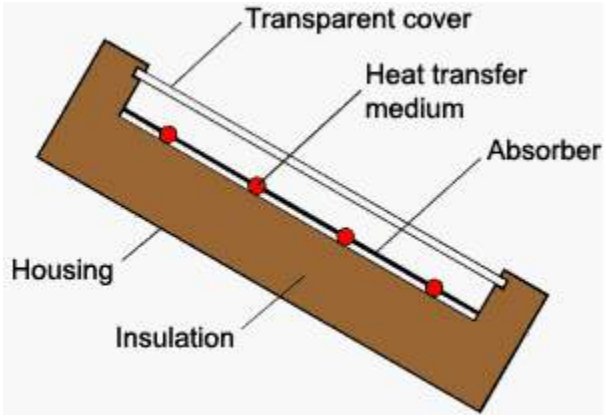

Figure 7.1. Sketch of the five nodes (7)

To find the governing equations of the model, energy balances were applied in both, the instantaneous HWS and components of the solar collector shown in Figure 6.1 and Figure 7.1 respectively.

7.1 Governing equations in the solar collector

The generic energy balance used to determine the differential equations in each part of the solar collector is given by the first law of thermodynamics, which dictates that the energy accumulated in the system is equal to the total net energy from the boundaries of a differential control volume:

$$\frac{dE}{dt} = \dot{Q}_{in} - \dot{Q}_{out} \quad (35)$$

Where,

$\frac{dE}{dt}$: Change in the internal energy
$\dot{Q}_{HWS}$: Heat transfer rate into the system from the boundaries
$\dot{Q}_{out}$: Heat transfer rate out of the system from the boundaries

In order to simplify the method, several assumptions were made (7):

- There is only no axial heat transfer for the solid elements or the fluid flow.

- The properties of the glass cover and insulation are constant, that is, independent of temperature; while the thermo- physical properties of the other zones, air gap, absorber and working fluid, are temperature dependent.
- The solar radiation (sky) and ambient conditions are time dependent.
- The sky can be considered as a black body for long- wavelength radiation at an equivalent sky temperature.

7.1.1 The glass cover

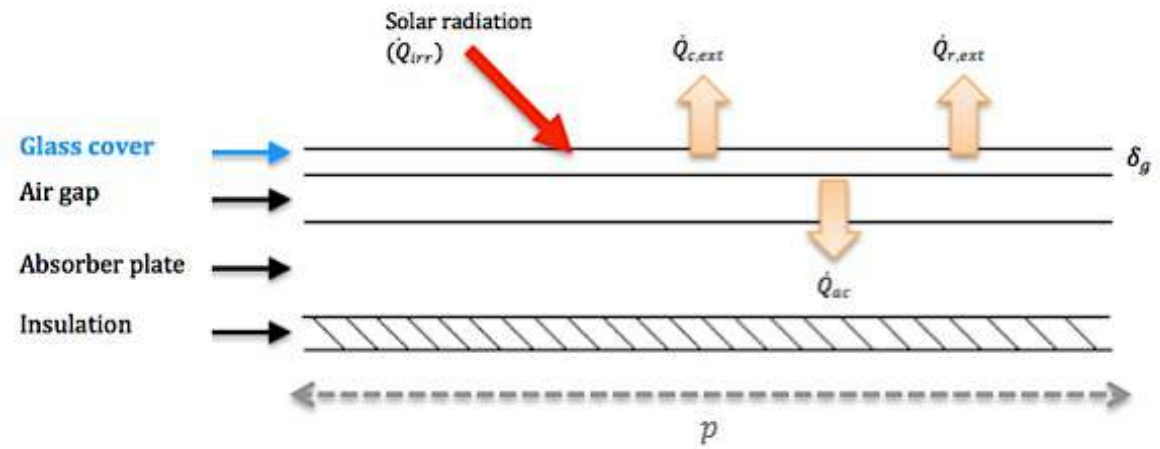

Figure 7.2. Energy balance in the glass cover

The cover absorbs energy through the heat radiated from solar irradiance, $\dot{Q}_{irr}$ (Equation (36)), and the heat transferred by convection from the working fluid circulating inside the collector,$\dot{Q}_{ac}$ (Equation (37)). (42)

$$\dot{Q}_{irr} = \alpha Q'' p \Delta z \qquad (36)$$

Where,

α: Absorption coefficient
p: Tube pitch
Δz: Spatial size of control volume (being $p\Delta z$ the area)

$$\dot{Q}_{ac} = h_{c,am-g}(T_{a,i} - T_g) p \Delta z \qquad (37)$$

Where,

$h_{c,am-g}$: Heat transfer coefficient between the ambient and the cover
$T_{a,i}$: Temperature of the air inside the solar collector
T_g: Temperature of the glass cover

Alternatively, the heat that flows out of the system is caused by natural convection to the surroundings, $\dot{Q}_{c,ext}$, (equation (38)) and heat radiated to the surroundings, $\dot{Q}_{r,ext}$ (equation (39)). (42)

$$\dot{Q}_{c,ext} = h_w(T_g - T_{am})p\Delta z \quad (38)$$

Where,

T_{am}: Ambient temperature

$$\dot{Q}_{r,ext} = h_{r,ext}(T_g - T_{am})p\Delta z \quad (39)$$

Where,

$h_{r,ext}$: Heat transfer coefficient by radiation to the surroundings

Hereby, substituting equations (36) to (39) into equation (35) can be deduced that,

$$c_g\rho_g V_g \frac{dT_g}{dt} = [\alpha Q'' + h_{c,am-g}(T_{am} - T_g) - h_w(T_g - T_a) - h_{r,ext}(T_g - T_{ab})]p\Delta z \quad (40)$$

Where,

c_g: Specific heat capacity of glass
ρ_g: Density of the glass cover
V_g: Volume of the glass cover
$\frac{dT_g}{dt}$: Variation of temperature of the glass cover with time

7.1.2 The air gap inside the collector

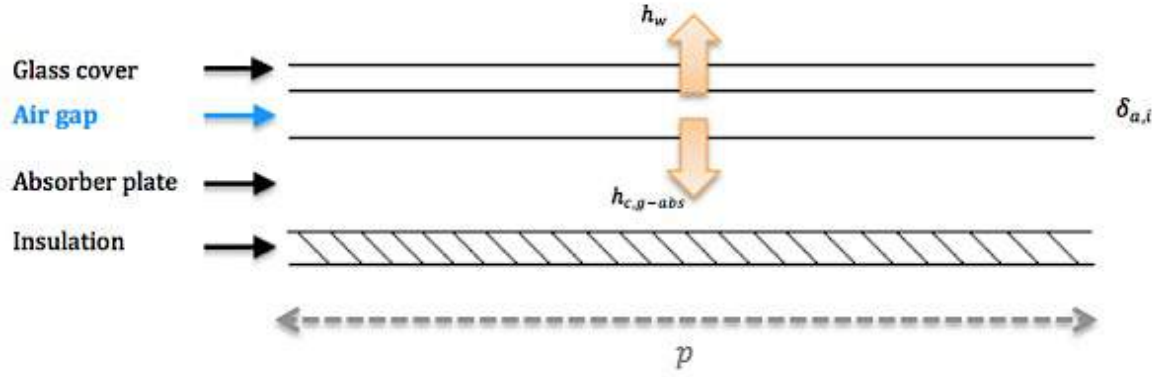

Figure 7.3. Energy balance in the air gap inside the collector

The air trapped between the absorber and the glass receives heat through the absorber plate by convection while, simultaneously, losing heat through the glass cover to the exterior (7). Thus, applying the principle stated in equation (35):

$$c_{a,i}(T_{a,i})\rho_{a,i}(T_{a,i})V_{a,i}\frac{dT_{a,i}}{dt} = \left[h_w\left(T_g - T_{a,i}\right) - h_{c,g-abs}(T_{a,i} - T_{abs})\right]p\Delta z \quad (41)$$

Where,

$c_{a,i}(T_{a,i})$: Specific heat capacity of air inside the collector (temperature dependent)
$\rho_{a,i}(T_{a,i})$: Density of air inside the collector (temperature dependent)
$V_{a,i}$: Volume of air inside the collector
$\frac{dT_{a,i}}{dt}$: Variation of air temperature inside the collector with time
$h_{c,g-abs}$: Heat transfer coefficient between the cover and the absorber
T_{abs}: Temperature of the absorber

7.1.3 The absorber plate

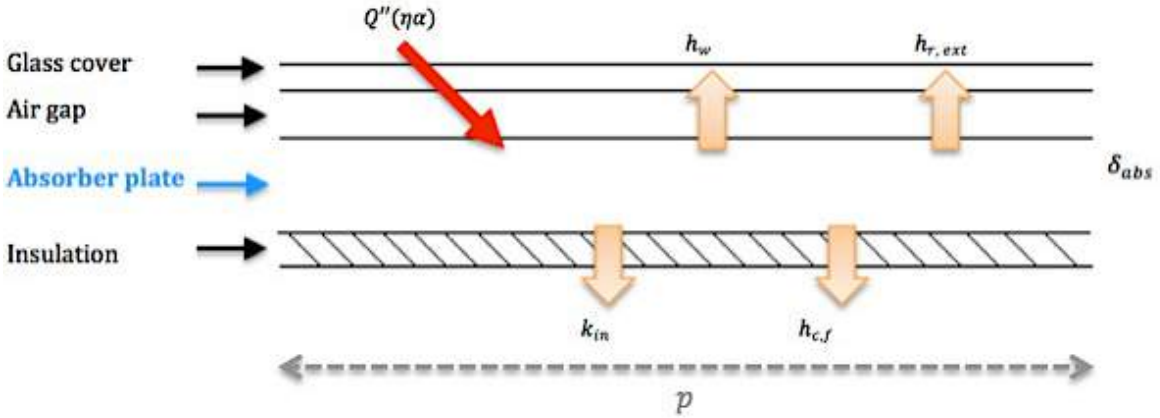

Figure 7.4. Energy balance in the absorber plate

This energy received by the absorber plate corresponds to the incident solar radiation, Q'', taking into account the absorption coefficient, α, the efficiency of the solar collector, η, and the plates surface (42).

$$\dot{Q}_{in} = Q''(\eta\alpha)p\Delta z \quad (42)$$

Where,

$(\eta\alpha)$: Effective transmittance- absorption coefficient

In contrast, the energy transferred from the absorber plate consists of the heat loss to the air inside the collector, the conduction between the absorber and the

insulation zone, the heat transfer to the glass cover through radiation, and lastly, the heat transfer by convection with the working fluid flow (7).

$$\dot{Q}_{out} = \left[h_w(T_{abs} - T_{a,i}) + \frac{k_{in}}{\delta_{in}}(T_{abs} - T_{in}) + h_{r,ext}(T_{abs} - T_i)\right] p\Delta z + \pi D_{in} h_{c,f} \Delta z (T_{abs} - T_{in}) \quad (43)$$

Where,

k_{in}: Insulation's thermal conductivity
δ_{in}: Insulation's thickness
T_{in}: Temperature at the insulation zone
$h_{c,f}$: Heat transfer coefficient of the working fluid

Therefore,

$$c_{abs}(T_{abs})\rho_{abs}(T_{abs})V_{abs}\frac{dT_{abs}}{dt} = \left\{Q''(\eta\alpha) - \left[h_w(T_{abs} - T_{a,i}) + \frac{k_{in}}{\delta_{in}}(T_{abs} - T_{in}) + h_{r,ext}(T_{abs} - T_i)\right]\right\} p\Delta z - \pi D_{in} h_{c,f} \Delta z (T_{abs} - T_{in}) \quad (44)$$

Where,

$c_{abs}(T_{abs})$: Specific heat capacity of the absorber plate (temperature dependent)
$\rho_{abs}(T_{abs})$: Density of the absorber (temperature dependent)
V_{abs}: Absorber's volume
$\frac{dT_{abs}}{dt}$: Variation of the absorber plate temperature with time

7.1.4 Insulation

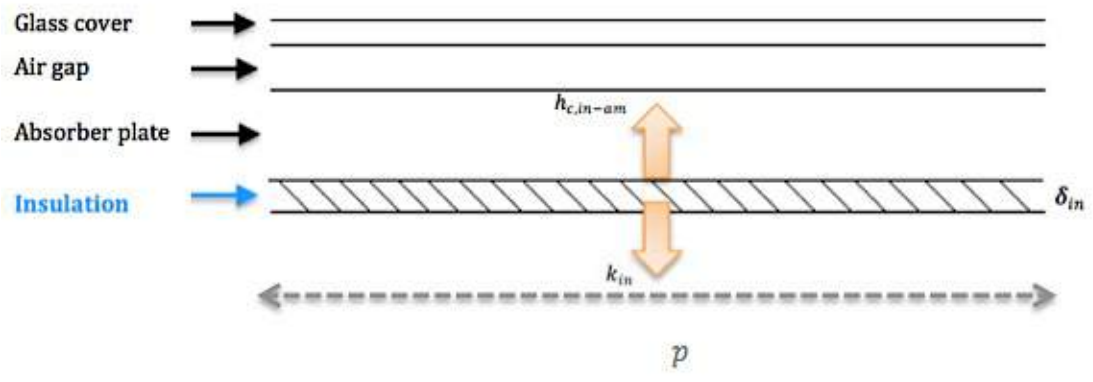

Figure 7.5. Energy balance in the insulation zone

The insulation zone of the solar collector transfers heat by conduction between the insulation and the absorber, and radiation through the bottom surface of the collector to the ambient. According to equation (35):

$$c_{in}\rho_{in}V_{in}\frac{dT_{in}}{dt} = \left[\frac{k_{in}}{\delta_{in}}(T_{abs} - T_{in}) - h_{c,in-am}(T_{in} - T_{amb})\right]p\Delta z \quad (45)$$

Where,

c_{in}: Specific heat capacity of the insulation material
ρ_{in}: Density of the insulation material
V_{in}: Volume of insulation
$\frac{dT_{in}}{dt}$: Variation of temperature of the insulation with time
$h_{c,in-am}$: Heat transfer coefficient between the insulation and the ambient

7.1.5 The working fluid

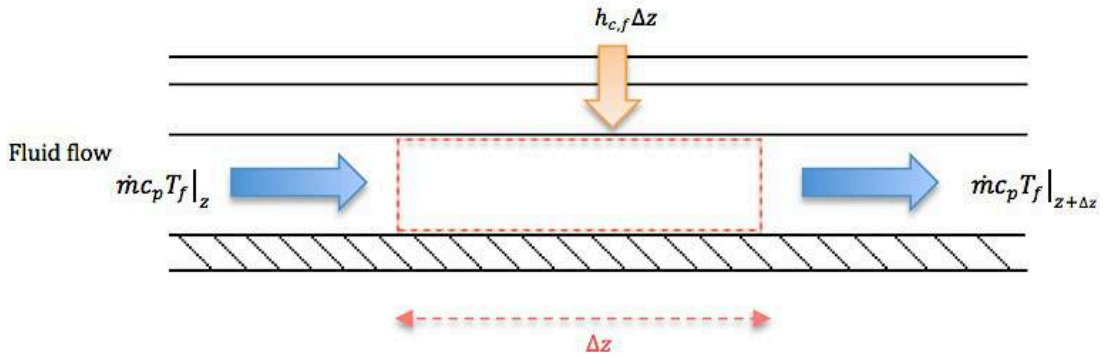

Figure 7.6. Energy balance in a control volume of the working fluid

Neglecting heat transfer conditions in the direction of the flow to simplify the model does not affect its validity; therefore, the energy balance of the working fluid can be written as (7):

$$c_f(T_f)\rho_f(T_f)A\frac{\delta T_f}{\delta t} = \pi D_{in}h_{c,f}(T_{abs} - T_{in}) - \dot{m}_f c_f(T_f)\frac{\delta T_f}{\delta z} \quad (46)$$

Where,

$c_f(T_f)$: Specific heat capacity of the working fluid (temperature dependent)
$\rho_f(T_f)$: Density of the absorber (temperature dependent)
A: Pipe's cross sectional area
$\frac{\delta T_f}{\delta t}$: Variation of the fluid's temperature with time
$h_{c,f}$: Heat transfer coefficient of the working fluid
$\dot{m}_f$: Mass flow rate of the working fluid
$\frac{\delta T_f}{\delta z}$: Variation of the fluid's temperature in the direction of the flow

7.2 The heat exchanger

The heat exchanger model is based on an energy balance between both circuits (HWS and refrigerant loop). Taking into account the efficiency of the heat exchanger stated in equation (10):

$$\varepsilon = \frac{q}{q_{max}}$$

Where q_{max} is the maximum energy that can be transferred in the heat exchanger:

$$q_{max} = C_{min}(T_{co} - T_{ci}) \quad (47)$$

In contrast, q is defined as follows:

$$q = C_{HWS}(T_{cons} - T_{net}) = C_{solar}(T_{ci} - T_{co}) \quad (48)$$

Where,

C_{HWS}: Heat capacity rate in circuit 2 (see Figure 6.1)
C_{solar}: Heat capacity rate in circuit 1 (see Figure 6.1)
C_{min} is defined as the smallest heat capacity rate between the one in circuit 1, C_{solar}, and circuit 2, C_{HWS}.

Finally, combining equations (47) and (48) the outlet temperatures for both, the HWS (Equation (49)) and the solar collector (Equation (50)):

$$\varepsilon = \frac{C_{HWS}(T_{cons} - T_{net})}{C_{min}(T_{co} - T_{ci})} \quad (49)$$

$$\varepsilon = \frac{C_{solar}(T_{ci} - T_{co})}{C_{min}(T_{co} - T_{ci})} \quad (50)$$

7.3 Summary of governing equations

Therefore, this are the simultaneous equations used to analyze the flow distribution in MATLAB:

i. Glass cover

$$c_g \rho_g V_g \frac{dT_g}{dt} = \left[\alpha Q'' + h_{c,am-g}(T_{am} - T_g) - h_w(T_g - T_a) - h_{r,ext}(T_g - T_{ab})\right] p \Delta z$$

ii. Air gap

$$c_{in} \rho_{in} V_{in} \frac{dT_{in}}{dt} = \left[\frac{k_{in}}{\delta_{in}}(T_{abs} - T_{in}) - h_{c,in-am}(T_{in} - T_{amb})\right] p \Delta z$$

iii. Absorber plate

$$c_{abs}(T_{abs}) \rho_{abs}(T_{abs}) V_{abs} \frac{dT_{abs}}{dt} =$$
$$= \left\{ Q''(\eta\alpha) - \left[h_w(T_{abs} - T_{a,i}) + \frac{k_{in}}{\delta_{in}}(T_{abs} - T_{in}) + h_{r,ext}(T_{abs} - T_i)\right]\right\} p \Delta z$$
$$- \pi D_{in} h_{c,f} \Delta z (T_{abs} - T_{in})$$

iv. Insulation

$$c_{in} \rho_{in} V_{in} \frac{dT_{in}}{dt} = \left[\frac{k_{in}}{\delta_{in}}(T_{abs} - T_{in}) - h_{c,in-am}(T_{in} - T_{amb})\right] p \Delta z$$

v. Working fluid

$$c_f(T_f) \rho_f(T_f) A \frac{\delta T_f}{\delta t} = \pi D_{in} h_{c,f}(T_{abs} - T_{in}) - \dot{m}_f c_f(T_f) \frac{\delta T_f}{\delta z}$$

vi. Heat exchanger

$$\varepsilon = \frac{C_{HWS}(T_{cons} - T_{net})}{C_{min}(T_{co} - T_{ci})}$$

$$\varepsilon = \frac{C_{solar}(T_{ci} - T_{co})}{C_{min}(T_{co} - T_{ci})}$$

8 RESULTS AND CONCLUSION

The research in this work was focused on the effect of flow distribution in manifolds arrangement in the sized flat plate solar collector. To do so, a proposed model implementing MATLAB software has been used based on an already existing model (7). The numerical model considers the transient behavior in an analyzed control volume of the flat plate solar collector, implementing the simultaneous equations stated in section 7.3. This chapter explains the results obtained from the study.

To understand the difference in behavior and consequences of a uniform versus a non- uniform flow distribution, the MATLAB code shown in Appendix A: MATLAB code was computed firstly for a uniform distribution of flow where the total flow rate of the system was divided by the number of tubes in the solar collector (Equation (51)), indicating thus, an evenly distribution throughout the headers of the solar collector. And secondly, for a non- uniform distribution of flow, introducing a vector, which described an increase in flow rate as the water from the header reached each tube.

$$flow = \frac{\dot{m}_s}{n} \tag{51}$$

Table 8.1 shows a summary of the data obtained from the sizing of the flat plate solar collector in section 6. Meanwhile, Table 8.2 describes the information obtained from section 4 regarding the HWS system configuration. Also, it is important to take into account that the solar global irradiance has been increased to 650 $Wh/_{m^2}$ instead of the value obtained in section 4.2.3 for the better understanding and significance of the results displayed in the numerical analysis. The rest of the parameters were kept constant from the original model due to the lack of information regarding their values.

GEOMETRY OF THE FLAT PLATE SOLAR COLLECTOR	
Internal diameter of the tubes	$6 \cdot 10^{-3} m$
Tube outer diameter	$7 \cdot 10^{-3} m$
Collectors' length	$1.8\ m$
Number of channels	13
Collector's width	$1.76\ m$

Table 8.1. Data regarding the geometry of the solar collector relevant for the study

OPERATING CONDITIONS	
Flow rate ($\dot{m}_s$)	$3.85\ {}^{kg}/_{s}$
HWS mass flow ($\dot{m}_c$)	$0.451\ {}^{kg}/_{s}$
Wind velocity	$2\ {}^{m}/_{s}$
Solar global radiation	$650\ {}^{Wh}/_{m^2}$
Ambient temperature	13.7°C

Table 8.2. Operating conditions used for the study

8.1 Results

Time (s)	**UNIFORM DISTRIBUTION OF FLOW** (°C)				**NON- UNIFORM DISTRIBUTION OF FLOW** (°C)			
	T_{net}	T_{co}	T_{ci}	$T_{co}-T_{ci}$	T_{net}	T_{co}	T_{ci}	$T_{co}-T_{ci}$
0	13	20	20	0	13	20	20	0
30	18,2607	20,0143	19,3827	0,6316	18,2583	20,0111	19,6162	0,3949
60	17,8375	19,45	18,8694	0,5806	17,9925	19,6567	19,2818	0,3749
90	17,4844	18,9792	18,441	0,5382	17,7606	19,3474	18,99	0,3574
120	17,1909	18,5879	18,085	0,5029	17,5589	19,0785	18,7363	0,3422
150	16,9481	18,2642	17,7905	0,4737	17,3841	18,8455	18,5164	0,3291
180	16,7485	17,998	17,5483	0,4497	17,2333	18,6444	18,3267	0,3177
210	16,5856	17,7808	17,3507	0,4301	17,1039	18,4719	18,1639	0,308
240	16,454	17,6053	17,191	0,4143	16,9935	18,3247	18,025	0,2997
270	16,3489	17,4652	17,0635	0,4017	16,9001	18,2001	17,9074	0,2927
330	16,2029	17,2706	16,8864	0,3842	16,8217	18,0956	17,8088	0,2868

Table 8.3. Results for both the uniform and non- uniform distribution of flow

Table 8.3 displays the results obtained from the MATLAB code for both configurations. This data has been interpreted using graphs, which will be explained in section.

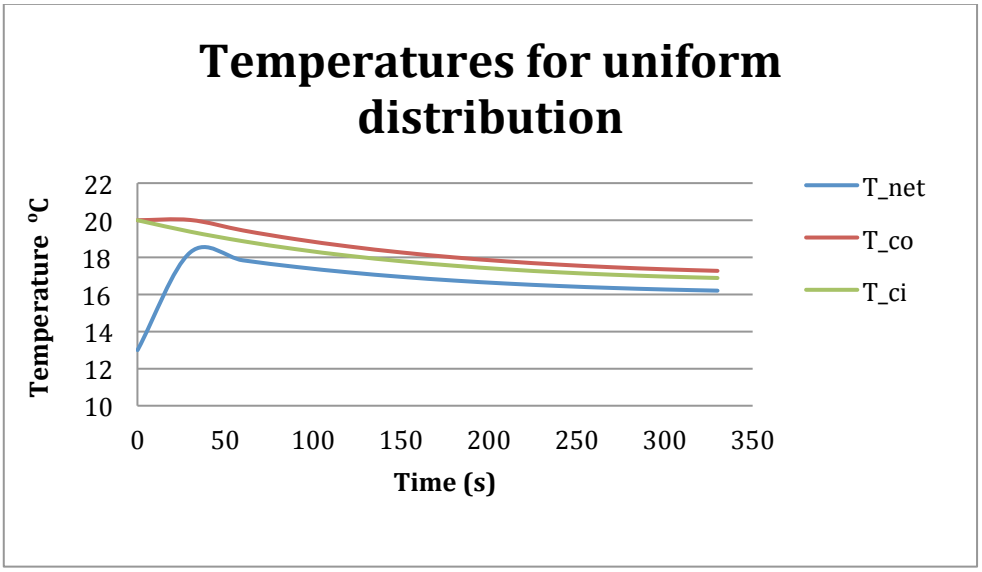

Figure 8.1. Graphical interpretation of the temperatures obtained for uniform distribution of flow

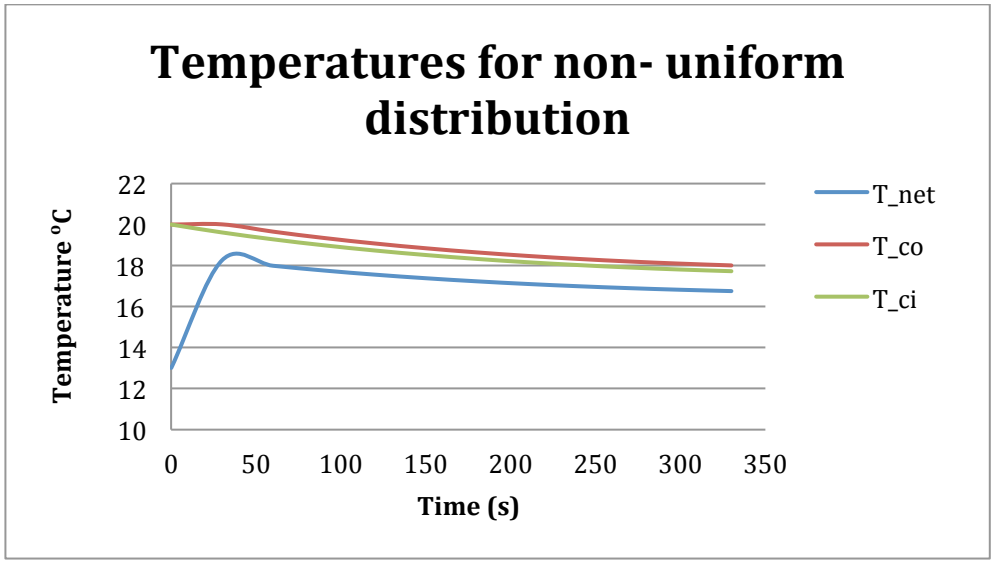

Figure 8.2. Graphical interpretation of the temperatures obtained for uniform distribution of flow

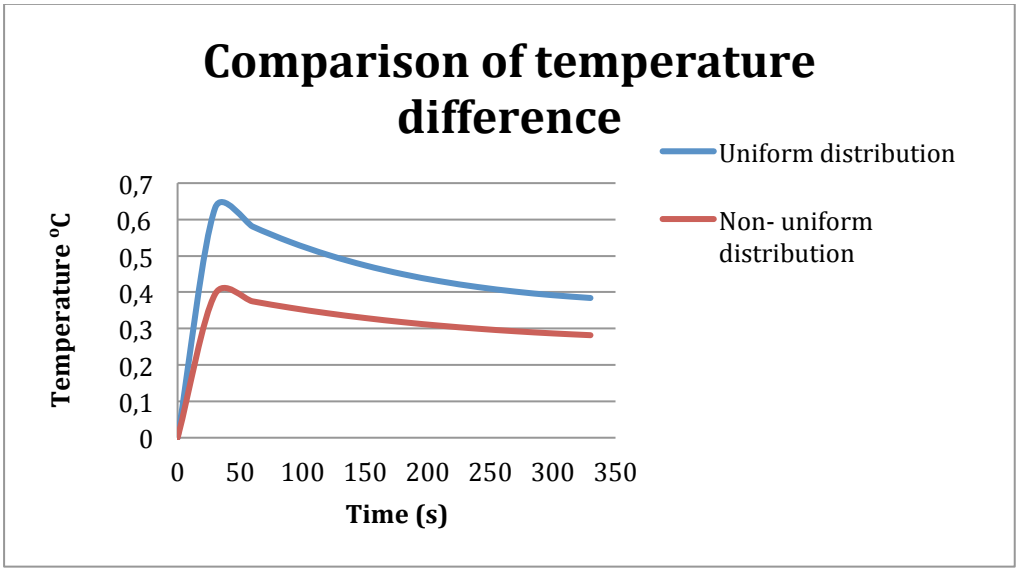

Figure 8.3. Comparison between two MATLAB configurations

The dimensionless parameters ϕ and β_i are introduced to study the flow distribution in the pipes (43):

$$\phi = \sqrt{\frac{\sum_{i=1}^{n}(\beta_i - \overline{\beta})}{n}} \quad (52)$$

Where,

ϕ: The non-uniformity
$\bar{\beta}$: The average flow ratio for the total tubes defined in equation (53)
β_i: The flow ratio for the ith tube defined in equation (54)

$$\bar{\beta} = \frac{\sum_{i=1}^{n}(\beta_i)}{N} \quad (53)$$

$$\beta_i = \frac{Q_i}{Q} \quad (54)$$

Therefore, according to equations (52), (53) and (54), if $\phi > 0$, the distribution of flow will not be uniform (43).

$$\boldsymbol{\phi = 0.0287491}$$

The result shows a non- uniformity in the distribution; but since this is an open scale, it does not quantify properly the misdistribution of flow in the pipes. Thus, other researches will have to be conducted changing different variables like for example, the flow rate; or using several collectors with different features, to

understand this value. In this case, the distribution can be in depth analyzed using the graphs obtained showing the effect that it has on temperature.

Although the graphs shown in Figure 8.1 and Figure 8.2 seem to be pretty similar or even identical, Figure 8.3 indicates that there is a difference between both models when comparing the temperature difference ($T_{co} - T_{ci}$). The graph shows that the more uniform the distribution is, the greater the temperature difference is. This occurs because uniform distributions of flow present uniform time of residence (defined as the average velocity divided by the length) in every channel; and consequently, an equal temperature in the tubes.

In the situation with the highest unbalance (first and last channel in this case) the channel with the lowest flux will hence have the lowest velocity and the greatest residence times. Subsequently, its temperature will be higher due to spending a larger amount of time inside the solar collector being exposed to solar radiation; but the outlet temperature will decrease as it is mixed with the manifold.

This behavior can be explained considering that the pipe with the lowest flux, gives the highest amount of temperature; therefore, as an adiabatic mixture is encountered when exiting the collector, the channels with the lowest temperatures will have the highest impact on the net temperature. As a result, it has been proven that these types of unbalances are undesirable for applications such as solar collectors.

On the other hand, the outlet temperature found with the numerical model reaches around 20°C, which is very low considering that consumption temperature is set at 45°C and the maximum temperature difference in the heat exchanger should not be higher than 5°C to avoid wear as explained in section 6.2.

Although lower water flows for HWS were tried, no relevant improvements were found in the changes; therefore, the system is not valid for this type of applications due to its incapability of heating up the water to the desired temperature; unless it is used as a preheater. Another alternative could be to use a storage tank to solve the problem, which was not in the scope of this work.

Finally, further studies could involve the use of a storage tank to correctly realize the HWS system as well as a more in detail study concerning this initiative.

8.2 Conclusions

Ultimately, according to the results obtained it can be concluded that:

- The solar collector has the following dimensions:

Area	$\mathbf{1.80 \times 1.76}\ (\boldsymbol{m^2})$
Number of tubes	13 $(D_i = 6mm;\ D_e = 7mm)$
Distance between tubes	13 cm

Table 8.4. Geometry of the solar collector

- The flow of consumption (Circuit 2) is:

$$\dot{m}_s = 3.85\ {}^{kg}/_{s}$$

- The flow in circuit 1 is:

$$\dot{m}_c = 0.541\ {}^{kg}/_{s}$$

- There is an unbalance in the distribution of flow inside the solar collector, which affects directly its efficiency demonstrated by lower outlet temperatures.

- A more accurate study considering the utilization of a storage tank will have to be done in order to properly incorporate this technology in the residence hall satisfying the corresponding demand.

9 BIBLIOGRAPHY

1. PIGFORD, Robert L., ASHRAF, Muhammad and MIRON, Yvon D. Flow distribution in piping manifolds. *Industrial & Engineering Chemistry Fundamentals* [online]. November 1983. Vol. 22, no. 4, p. 463–471. [Accessed 7 September 2016]. DOI 10.1021/i100012a019. Available from: http://pubs.acs.org/doi/abs/10.1021/i100012a019
2. WANG, Junye. Theory of flow distribution in manifolds. *Chemical Engineering Journal*. 2011. Vol. 168, no. 3, p. 1331–1345. DOI 10.1016/j.cej.2011.02.050.
3. LÓPEZ, R and LECUONA, a. A Numerical Procedure for Flow Distribution and Pressure Drops for U and Z Type Configurations Plate Heat Exchangers with Variable Coefficients. *Journal of Physics: …* [online]. 2012. Vol. 12060, no. iii. DOI 10.1088/1742-6596/395/1/012060. Available from: http://iopscience.iop.org/1742-6596/395/1/012060
4. BASSIOUNY, M.K. and MARTIN, H. Flow distribution and pressure drop in plate heat exchangers. *Journal of Chemical Information and Modeling*. 2013. Vol. 53, no. 9, p. 1689–1699. DOI 10.1017/CBO9781107415324.004.
5. WANG, Junye. Pressure drop and flow distribution in parallel-channel configurations of fuel cells: U-type arrangement. *International Journal of Hydrogen Energy* [online]. 2008. Vol. 33, no. 21, p. 6339–6350. DOI 10.1016/j.ijhydene.2008.08.020. Available from: http://dx.doi.org/10.1016/j.ijhydene.2008.08.020
6. WANG, Junye. Pressure drop and flow distribution in parallel-channel configurations of fuel cells: Z-type arrangement. *International Journal of Hydrogen Energy* [online]. 2010. Vol. 35, no. 11, p. 5498–5509. DOI 10.1016/j.ijhydene.2010.02.131. Available from: http://dx.doi.org/10.1016/j.ijhydene.2010.02.131
7. SALEH, Ahmad M. *Modeling of flat- plate solar collector operation in transient states*. Purdue University, 2012.
8. GOBIERNO DE ESPAÑA. *Documento básico HE ahorro de energía* [online]. 2013. ISBN RD 314/2006 - Orden FOM/163/2013. Available from: http://www.codigotecnico.org/web/recursos/documentos/
9. Energía solar- Twenergy. [online]. Available from: https://twenergy.com/energia/energia-solar
10. The history of solar energy. [online]. [Accessed 9 July 2016]. Available from: https://www1.eere.energy.gov/solar/pdfs/solar_timeline.pdf
11. La energía solar. [online]. [Accessed 9 July 2016]. Available from: http://www.censolar.es/menu2.htm

12. RADIANTEC. What is the best type of solar collector for my application? [online]. Available from: http://www.radiantsolar.com/FAQs/FAQbestsolarcollector.php

13. Advantages and Disadvantages of Solar Energy | GreenMatch.co.uk. [online]. Available from: http://www.greenmatch.co.uk/blog/2014/08/5-advantages-and-5-disadvantages-of-solar-energy

14. Energía solar térmica tecnologías y aplicaciones. [online]. 2014. [Accessed 10 September 2016]. Available from: http://www.renewables-made-in-germany.com/es/renewables-made-in-germany/tecnologias/energia-solar-termica/energia-solar-termica/tecnologias-y-aplicaciones.html

15. Solar Thermal Energy. [online]. Available from: http://es.slideshare.net/Rosalmara/solar-thermal-energy-isabel

16. Instalaciones Termosolares para la Producción de Agua Caliente Sanitaria (ACS). [online]. Available from: http://ingemecanica.com/tutorialsemanal/tutorialn188.html#seccion23

17. PENNSYLVANIA SOLAR COURSE. Solar Hot Water Basics. [online]. Available from: http://www.pasolar.ncat.org/lesson02.php#types

18. ASOCIACIÓN TÉCNICA ESPAÑOLA DE CLIMATIZACIÓN Y REFRIGERACIÓN. *Guía técnica de agua caliente sanitaria central* [online]. 2010. ISBN 9788496680524. Available from: www.idae.es

19. Hot water service. [online]. Available from: http://www.yourhome.gov.au/energy/hot-water-service

20. GUPTA, Bipin. Solar flat plate collector. *9th of February* [online]. 2015. Available from: http://es.slideshare.net/bgiuppitna/solar-tube-collectorDesign, Fabrication and Testing of Flat Plate Solar Thermal Collector

21. JONES, Ben. Flat Plate Solar Thermal Collectors: Overview - The Green Home. [online]. Available from: http://thegreenhome.co.uk/heating-renewables/solar-panels/flat-plate-solar-thermal-collectors-overview/

22. Solar Geyser Technology Explained. [online]. Available from: http://www.solarsense.co.za/solar-water-heating-explained.php

23. Components of a Flat-Plate Solar Collector. [online]. Available from: http://www.energy.kth.se/compedu/webcompedu/WebHelp/S9_Renewable_Energy/B5_Solar_Energy/C3_Advanced_Solar_Thermal/ID107_files/Components_of_a_Flat-Plate_Solar_Collector.htm

24. Solar Collectors: Different types and Fields of Application. . Solar collectors, specialized technical informations

25. *Research Institute for Sustainable Energy* [online]. RISE, Murdoch University. [Accessed 8 September 2016]. Available from: https://web.archive.org/web/20110309140814/http://www.rise.org.au/info/Tech/lowtemp/hotwatersys.html

26. BALLESTEROS RUIZ, Maite. *Análisis de métodos de dimensionado de instalaciones solares para ACS.* [online]. 2012. [Accessed 8 September 2016]. Available from: http://e-archivo.uc3m.es/bitstream/handle/10016/17045/PFC - Maite Ballesteros Ruiz.pdf?sequence=1
27. EUROPEAN'S COMMISION (JRC). Geographic Information System. [online]. Available from: http://re.jrc.ec.europa.eu/pvgis/apps4/pvest.php?lang=es&map=europe
28. NASA. Solar Radiation and the Earth System. [online]. Available from: http://education.gsfc.nasa.gov/experimental/July61999siteupdate/inv99Project.Site/Pages/science-briefs/ed-stickler/ed-irradiance.html
29. SANCHO, Jm, RIESCO, J and JIMÉNEZ, C. *Atlas de Radiación Solar en España utilizando datos del SAF de Clima de EUMETSAT* [online]. 2012. Available from: http://scholar.google.com/scholar?hl=en&btnG=Search&q=intitle:Atlas+de+Radiación+Solar+en+España+utilizando+datos+del+SAF+de+Clima+de+EUMETSAT#0Radiación solar
30. Clima Madrid. [online]. Available from: http://www.climatedata.eu/climate.php?loc=spxx0050&lang=es
31. INSTITUTO PARA LA DIVERSIFICACIÓN Y AHORRO DE LA ENERGÍA (IDAE). *Pliego de Condiciones Técnicas de Instalaciones a Baja Temperatura*. 2009.
32. The Effect of Azimuth Angle on Energy Output | CivicSolar. [online]. Available from: https://www.civicsolar.com/support/installer/articles/effect-azimuth-angle-energy-output
33. Collector Orientation | EME 810: Solar Resource Assessment and Economics. [online]. Available from: https://www.e-education.psu.edu/eme810/node/576
34. ARIAS, Luis Platón, JULIO, D, SAN, Francisco and ALONSO, José. Optimización del dimensionado de instalaciones de energía solar térmica para producción de agua caliente sanitaria.
35. Funcionamiento de la energía solar térmica | Ekidom S.L. Energías Renovables en Bizkaia, Gipuzkoa y Alava. [online]. Available from: http://www.ekidom.com/funcionamiento-de-la-energia-solar-termica
36. FUENTES CANTERO, David. *Instalación de colectores solares para suministro de ACS en Valencia* [online]. [no date]. [Accessed 8 September 2016]. Available from: http://e-archivo.uc3m.es/bitstream/handle/10016/7794/PFC_David_Fuentes_Cantero.pdf?sequence=1
37. BERGMAN, Theodore L., LAVINE, Adrienne S., INCROPERA, Frank P and DEWITT, David P. *Fundamentals of Heat and Mass Transfer*. Seventh. 2007. ISBN 13 978-0470-50197-9.

38. AGARWAL, V. K. and LARSON, D. C. *Calculation of the top loss coefficient of a flat-plate collector*. 1981.

39. DUFFIE, J. a., BECKMAN, William a. and WOREK, W. M. *Solar Engineering of Thermal Processes, 4nd ed.* [online]. 2003. ISBN 1118418123. Available from: http://books.google.com/books?hl=en&lr=&id=qkaWBrOuAEgC&pgis=1

40. CERÓN, Juan F. *Análisis del mecanismo de transferencia de calor en colectores solares térmicos y de la influencia de las condiciones de contorno* [online]. 2012. Available from: http://repositorio.bib.upct.es/dspace/bitstream/10317/2885/1/pfc4460.pdf

41. GUEVARA VÁSQUES, Sixto. *Teoría para el diseño de calentadores solares de agua* [online]. Lima, 2003. [Accessed 22 September 2016]. Available from: http://www.bvsde.ops-oms.org/tecapro/documentos/miscela/iTeoriacalienta.pdf

42. FAN, Jianhua, SHAH, Louise Jivan and FURBO, Simon. FLow distribution in a solar collector panel with horizontally inclined absorber strips. In : *Solar Energy* [online]. 2007. [Accessed 13 September 2016]. ISBN 1815-5901. Available from: http://scielo.sld.cu/pdf/rie/v36n3/rie07315.pdf

43. HASSAN, Jafar M., MOHAMED, Thamer A., MOHAMMED, Wahid S., ALAWEE, Wissam H., HASSAN, Jafar M., MOHAMED, Thamer A., MOHAMMED, Wahid S. and ALAWEE, Wissam H. Modeling the Uniformity of Manifold with Various Configurations. *Journal of Fluids* [online]. 2014. Vol. 2014, p. 1–8. [Accessed 16 September 2016]. DOI 10.1155/2014/325259. Available from: http://www.hindawi.com/journals/fluids/2014/325259/

10 APPENDICES

10.1 Appendix A: MATLAB code

```
clc
clear all
global Fc T_acs_i m_acs Cp_acs ef t_inicial
global p d_in r_o r_in A delta_g delta_i delta_ab delta_a c_g c_i rho_g
global rho_i alpha tau_alpha K_i c_ab rho_ab c_a L
global mdot w_f dtau

%%%%%%%%%%%%%%%%%%%%%% INTRODUCED BY THE USER %%%%%%%%%%%%%%%%%%%%%%%%%%%%
%--------------------------- GEOMETRY -------------------------------------
p=1.76;               %tube pitch (m)
d_in=6/1000;          %tube inner diameter(m)
d_o=7/1000;           %tube outer diameter (m)
r_o=d_o/2;            %tube outer radius(m)
r_in=d_in/2;          %tube inner radius(m)
A=pi*r_in^2;          %flow area(sqm)

%------------------------------PARAMETERS---------------------------------
delta_g=3.81/1000;    %cover thickness
delta_i=50.8/1000;    %insulation thickness(m)
delta_ab=.015;        %absorber thickness(m)
delta_a=.025;         %air gap thickness(m)
c_g=720;              %cover specific heat (J/kg.K)
c_i=1030;             %insulation specific heat (J/kg.K)
rho_g=2500;           %cover density(Kg/m^3)
rho_i=70;             %insulation density(Kg/m^3)
alpha=.005;           %absorption coefficient;
tau_alpha=.861;       %effictive transmittance-absorption coef.
K_i=0.035;            %insulation thermal conductivity(W/m.K)
c_ab =385;            %absorber specific heat (J/kg.K)
rho_ab =8795;         %absorber density(Kg/m^3)
c_a=1.0056e+003;      %air specific heat (J/kg.K)
%------------------------------------------------------------------------
%------------------------------------------------------------------------
Fc=10;                                        %Parametro regulador del paso de
tiempo
L=1.8;                                        %length of tubes (m)
%%%%%%%%%%%%%%%%%%%%%%%%%%%%%%%%%%%%%%%%%%%%%%%%%%%%%%%%%%%%%%%%%%%%%%%%%%%
n=4;                                          %NUMBER OF NODES
flowrate=61.02;                               %TOTAL FLUX IN GPM
interval=5;                                   %total running time (min)
initialtemp=20;                               %INITIAL TEMPERATURE
Nt=13;                                        % NUMBER OF CHANNELS

%-------------FLOW DISTRIBUTION IN THE SOLAR COLLECTOR---------------------
%Uniform:
%flow(1:Nt,1)=flowrate/Nt;
%fluid volume flow rate per tube (GPM)

%OR

%Non- uniform:
flow=[4.69 5.159 5.628 6.097 6.566 7.035 7.504 7.973 8.442 8.911 9.38 9.849
10.318];  %fluid volume flow rate per tube (GPM)

%%%%%%%%%%%%%%%%%%%%%%%%%%%%%%%%%%%%%%%%%%%%%%%%%%%%%%%%%%%%%%%%%%%%%%%%%%%

Vdot(1:Nt,1)=flow/15852;                      %fluid volume flow rate (m^3/s)
```

```
mdot=Vdot*1000;                              %fluid mass flow rate (Kg/s)
w_f=4*Vdot/(pi*d_in^2);                      %working fluid velocity
dtau=30;                                     % paso de tiempo (s)
%--------------------------- HWS SYSTEM ----------------------------------
T_acs_i=13;                          %Temperature of network water in HWS (ºC)
m_acs=0.451;                         %mass flow of water in the HWS (kg/s)
Cp_acs=4.18;                         %Cp water (kJ/(kg*K)
ef=0.75;                             %Collector's efficiency

%--------------------------SOLAR COLLECTOR -------------------------------

t_inicial=20;                      %Initial temperature (ºC)
[tiempo,Tsal,T_ent_panel,Tsal_acs]=results_4(n,Nt,flowrate,interval,initialtem
p);

hold on
plot(tiempo,Tsal_acs,'-r')
plot(tiempo,Tsal,'-b')
plot(tiempo,T_ent_panel,'-g')

%[tiempo Tsal_acs Tsal T_ent_panel]
```

```
function  [ny_a,alpha_a,k_a] = air_prop(t_a)
T_vec=[250 300 350 400 450];
ny_vec = [11.44 15.89 20.92 26.41 32.39]*1E-6;
alpha_vec = [15.9 22.5 29.9 38.3 47.2]*1E-6;
ka_vec = [22.3 26.3 30.0 33.8 37.3]*1E-3;
ny_a = interp1(T_vec,ny_vec,t_a,'spline');
alpha_a = interp1(T_vec,alpha_vec,t_a,'spline');
k_a = interp1(T_vec,ka_vec,t_a,'spline');
```

```
function
[Bx,Cx,Dx,Ex,Fx,Gx,Hx,Kx,Lx,Mx,Ox,Px,Qx,Rx,Sx,Ux,Vx,Wx,Xx,Jx]=coeff_4(t_g,t_a,
t_ab,t_f,t_i,t_am,dtau,dz,n,mdot,k,w_f)
global c_f
global p d_in r_o r_in A delta_g delta_i delta_ab delta_a c_g c_i rho_g
global rho_i alpha tau_alpha K_i c_ab rho_ab c_a

%Coefficients of the transiant temperature equations.

[h_g_am, h_r1, h_c1, h_f, h_i_am]=
get_h(t_f,t_a,t_g,t_ab,t_i,n,t_am,delta_a,d_in,k,w_f);
[rho_a] = rho(t_a);
[rho_f,c_f]= waterprop(t_f);


Bx=h_g_am/(c_g*rho_g*delta_g);
Cx=h_r1/(c_g*rho_g*delta_g);
Dx=h_c1/(c_g*rho_g*delta_g);
Ex=alpha/(c_g*rho_g*delta_g);
Fx=(1/dtau)+Bx+Cx+Dx;
Jx=c_ab*rho_ab*(p*delta_ab+pi*(r_o^2-r_in^2));
Kx=p*(tau_alpha)./Jx;
Lx=h_r1*p./Jx;
Mx=h_c1*p./Jx;
Ox=pi*d_in*h_f./Jx;
Px=p*K_i./(Jx*delta_i);
Gx=h_c1*p./(c_a*rho_a*(p*delta_a-pi*r_o^2));
```

```
Hx=(1/dtau)+(2*Gx);
Qx=(1/dtau)+Lx+Mx+Ox+Px;
Rx=pi*d_in*h_f./(c_f.*rho_f*A);
Sx=mdot./(rho_f*A);
Ux=(1/dtau)+Rx+(Sx/dz);
Vx=2*K_i/(c_i*rho_i*delta_i^2);
Wx=2*h_i_am./(c_i*rho_i*delta_i);
Xx=(1/dtau)+Vx+Wx;
```

```
function
[h_g_am,h_r1,h_c1,h_f,h_i_am]=get_h(t_f,t_a,t_g,t_ab,t_i,n,t_am,delta_a,d_in,k
,w_f)
[ny_a,alpha_a,k_a] = air_prop(t_a);
[k_f,ny_f,Pr_f]=kf(t_f);
Re_f=w_f.*d_in./ny_f;

segma=5.6697*10^-8;
emi_g=.88;emi_ab=.1;emi_i=.05;
g=9.81;
theta=(pi/4);       %tilt angle
a=1.8;b=1.76;L=a;    %collector dimensions
U_inf=2;          %wind velocity

%%%%

h_f=zeros(n,1);h_r1=zeros(n,1);h_c1=zeros(n,1);h_g_am=zeros(n,1);
h_i_am=zeros(n,1);Nu_f=zeros(n,1);Nu_a=zeros(n,1);Ra=zeros(n,1);
ny_am =1.5743*10^-5;
k_am=.0262;         %ambiant thermal conductivity
Pr_am=0.71432;      %ambiant Prandtl number

delta=4*a*b/sqrt(a^2+b^2);
Re_am=U_inf*delta/ny_am;
Nu_am=.86*Re_am^.5*Pr_am^(1/3);
h_c2=Nu_am*k_am/delta;

%%%%

t_sky=.0552.*t_am.^1.5;
Nu_f=4.4+(.00398.*(Re_f.*Pr_f.*(d_in/L)).^1.66./(1+.0114.*(Re_f.*Pr_f.*(d_in/L
)).^1.12));
h_f=Nu_f.*k_f./d_in;

for j=1:n
    Ra(j)=abs(t_g(j)-t_ab(j))*g*delta_a^3/(ny_a(j)*alpha_a(j)*t_a(j));
    AA=1-(1708/(Ra(j)*cos(theta)));
    BB=(Ra(j)*cos(theta)/5830)^(1/3)-1;
    if AA<=0
        if BB<=0
          Nu_a(j)=1;
        else Nu_a(j)=1+BB;
        end
    else if BB<=0
            Nu_a(j)=1+(1.44*(1-
(1708*(sin(1.8*theta))^1.6/(Ra(j)*cos(theta))))*AA);
        else Nu_a(j)=1+(1.44*(1-
(1708*(sin(1.8*theta))^1.6/(Ra(j)*cos(theta))))*AA)+BB;
        end
    end
h_r1(j)=(segma*(t_ab(j)^2+t_g(j)^2)*(t_ab(j)+t_g(j)))/((1/emi_ab)+(1/emi_g)-
1);
h_c1(j)=Nu_a(j)*k_a(j)/delta_a;
```

```
if t_g(j)-t_am(k)==0
    h_g_am(j)=h_c2;
else h_g_am(j)=((segma*emi_g*(t_g(j)^4-t_sky(k)^4))/(t_g(j)-t_am(k)))+h_c2;
end
if  t_i(j)-t_am(k)==0
    h_i_am=h_c2;
else
    h_i_am(j)=((segma*emi_i*(t_i(j)^4-t_sky(k)^4))/(t_i(j)-t_am(k)))+h_c2;
end

end
```

```
function [k_f,ny_f,Pr_f]=kf(t_f)
T_vec = [273.15 300 350];
kf_vec = [0.57214 0.61497 0.66786 ];
nyf_vec = [1.6438E-6 8.3610E-7 3.6987E-7];
Prf_vec = [11.822 5.5141 2.1929];
k_f = interp1(T_vec,kf_vec,t_f,'spline');
ny_f = interp1(T_vec,nyf_vec,t_f,'spline');
Pr_f = interp1(T_vec,Prf_vec,t_f,'spline');
```

```
function [rho_a] = rho(t_a)
T_vec = [250 300 350 400 450];
rho_vec = [1.4235 1.1771 1.0085 0.88213 .8770];
rho_a=interp1(T_vec,rho_vec,t_a,'spline');
```

```
function  [rho_f,c_f]= waterprop(t_f)
T_vec = [273.15 300 350];
rhof_vec = [1000.4 996.75 973.8];
cf_vec = [4112.9 4071.7 4068.5];
rho_f = interp1(T_vec,rhof_vec,t_f,'spline');
c_f = interp1(T_vec,cf_vec,t_f,'spline');
```

```
function
[tiempo,Tsal,T_ent_panel,Tsal_acs]=results_4(n,Nt,flowrate,interval,initialtem
p)
global Fc T_acs_i m_acs Cp_acs  ef t_inicial
global c_f
global p d_in r_o r_in A delta_g delta_i delta_ab delta_a c_g c_i rho_g
global rho_i alpha tau_alpha K_i c_ab rho_ab c_a L
global mdot w_f dtau
tic
kmax=500;  TOLcor=1e-3;

ts= cputime;                                %time at the function start
dz=L/(n-1);                                 %spatial step (m)
Zc=linspace(0,L,n)';

T_tot=interval*60/dtau+1;
```

```
disp(['The number of time steps is= ' num2str(T_tot)])

pause

t_am=zeros(T_tot+1,1);                          %Ambient temp.
G_r=zeros(T_tot+1,1);                           %heat flux of solar radiation
(W/sqm)
t_g=ones(n,Nt)*(t_inicial+273.15);              %initial glass temp.
t_a=ones(n,Nt)*(t_inicial+273.15);              %initial air gap temp.
t_ab=ones(n,Nt)*(t_inicial+273.15);             %initial absorber temp.
t_f=ones(n,Nt)*(t_inicial+273.15);              %initial fluid temp.
t_i=ones(n,Nt)*(t_inicial+273.15);              %initial insulation temp.
Tsal=(t_inicial)*ones(T_tot+1,1);
Tsal_acs=(T_acs_i)*ones(T_tot+1,1);
T_ent_panel=t_inicial*ones(T_tot+1,1);

t_gc=zeros(T_tot,1);t_ac=zeros(T_tot,1);t_abc=zeros(T_tot,1);
t_fc=zeros(T_tot,1);t_ic=zeros(T_tot,1);t_out=zeros(T_tot,1);

tiempo=zeros(T_tot+1,1);
Q_dot=zeros(T_tot,1);

%------ INITIALIZATION OF SOLAR RADIATION AND AMBIENT TEMPERATURES --------
%%loop in secods
for k=1:T_tot+1
    G_r(k)=650;                                 %Solar Radiation (W/m2)
    t_am(k)=13.7+273.15;
end
%-------------------------------------------------------------------------
t_f(1,:)=20+273.15;

for k = 1:T_tot
    disp(k)
    tiempo(k+1,1)=tiempo(k,1)+dtau;
    n_converge=0;

    for r=1:Nt

        %---------------------- TEMPERATURAS EN n ---------------------------
        t_g_old=t_g(:,r);           % GLASS COVER TEMPERATURE
        t_a_old=t_a(:,r);           % AIR GAP TEMPERATURE
        t_ab_old=t_ab(:,r);         % ABSORBER TEMPERATURE
        t_f_old=t_f(:,r);           % FLUID TEMPERATURE
        t_i_old=t_i(:,r);           % INSULATION TEMPERATURE

        kk=0; Error=1;
        while Error>=TOLcor && k<kmax

            t_g_2=t_g(:,r);         % GLASS COVER TEMPERATURE
            t_a_2=t_a(:,r);         % AIR GAP TEMPERATURE
            t_ab_2=t_ab(:,r);       % ABSORBER TEMPERATURE
            t_f_2=t_f(:,r);         % FLUID TEMPERATURE
            t_i_2=t_i(:,r);


[Bx,Cx,Dx,Ex,Fx,Gx,Hx,Kx,Lx,Mx,Ox,Px,Qx,Rx,Sx,Ux,Vx,Wx,Xx,Jx]=coeff_4(t_g(:,r)
,t_a(:,r),...

t_ab(:,r),t_f(:,r),t_i(:,r),t_am,dtau,dz,n,mdot(r,1),k,w_f(r,1));

            t_g(:,r)=((t_g_old/dtau)+(Bx*t_am(k))+(Cx.*t_ab(1,r))...
                +(Dx.*t_a(:,r))+(Ex*G_r(k))./Fx;

            t_a(:,r)=((t_a_old/dtau)+(Gx.*(t_g(:,r)+t_ab(:,r)))./Hx;
```

```
t_ab(:,r)=((t_ab_old/dtau)+(Kx*G_r(k))+(Lx.*t_g(:,r))+(Mx.*t_a(:,r))+(Ox.*t_f(
:,r))...
                +(Px.*t_i(:,r))./Qx;

            t_f(1,r)=T_ent_panel(k,1)+273.15;


t_f(2:n,r)=((t_f_old(2:n)/dtau)+(Rx(2:n).*t_ab(2:n,r))+(Sx(2:n).*t_f(1:n-
1,r)/dz))./Ux(2:n);

            t_i(:,r)=((t_i_old/dtau)+(Vx.*t_ab(:,r))+(Wx(:)*t_am(k)))./Xx;

            Error=100*max([max(abs(t_g(:,r)-t_g_2(:))./t_g_2(:));...
                           max(abs(t_a(:,r)-t_a_2(:))./t_a_2(:));...
                           max(abs(t_ab(:,r)-t_ab_2(:))./t_ab_2(:));...
                           max(abs(t_i(:,r)-t_i_2(:))./t_i_2(:));...
                           max(abs(t_f(:,r)-t_f_2(:))./t_f_2(:))]);
        end

    end


    Tsal(k+1,1)=sum(mdot.*(t_f(end,:)'))/sum(mdot)-273.15;

    [~,c_f]= waterprop(Tsal(k+1,1)+273.15);

    Ch=sum(mdot)*c_f;
    Cc=1000*m_acs*Cp_acs;

    Cmin=min(Ch,Cc);
    DTmax=Tsal(k+1,1)-T_acs_i;
    qmax=Cmin*DTmax;

    t_f(1,:)=Tsal(k+1,1)+273.15-ef*qmax/Ch;
    T_ent_panel(k+1,1)=t_f(1,1)-273.15;
    Tsal_acs(k+1,1)=ef*qmax/Cc+T_acs_i;

end
toc
```